2023

The Analysis, Development and Calibration of Prototype Hardware in Effort to Improve Brake Thermal Efficiency and Real-World Fuel Economy of the International Supertruck

Matthew Taylor
Minnesota State University, Mankato

The Analysis, Development and Calibration of Prototype Hardware in Effort to Improve Brake Thermal Efficiency and Real-World Fuel Economy of the International Supertruck

By

Matthew Taylor

A Thesis Submitted in Partial Fulfillment of the

Requirements for the Degree of

Master of Science

In

Manufacturing Engineering Technology

Concentration: Automotive Engineering

Minnesota State University, Mankato

Mankato, Minnesota

November 2023

November 15, 2023

The Development and Calibration of Prototype Hardware in Effort to Improve Brake Thermal Efficiency and Real-World Fuel Mileage of the International Supertruck

Matthew Taylor

This thesis has been examined and approved by the following members of the student's committee.

_____

Gary Mead - Advisor

_____

Dennis Soltis - Committee Member

_____

Kuldeep Agarwal - Committee Member

TABLE OF CONTENTS

CHAPTER

      CHAPTER 1 – THERMODYNAMICS, FRICTION, AND DOWNSPEEDING

      CHAPTER 2 – BOWL NOZZLE CONFIGURATION

      CHAPTER 3 – TURBOCHARGER SELECTION

      CHAPTER 4 – VARIABLE WATER PUMP

FINAL RESULTS AND SUMMARY

REFERENCES

<u>Acknowledgement</u>

List of Figures

List of Equations

Acronyms and Abbreviations:

13M (13 mode): The steady-state point test of the RMC points.

AFR: Air fuel Ratio

BMEP: Brake Mean Effective Pressure (bar)

BSFC: Brake Specific Fuel Consumption (lb/hp-hr)

bTDC: Before Top-Dead Center

BTE: Brake Thermal Efficiency (%)

CA10: 10% Mass burn fraction (deg Crs)

CA10-90: Cumulative Mass burn fraction (deg Crs)

C_p: Specific heat at constant pressure

CR: Compression Ratio

C_v: Specific heat at constant volume

Deg Crs: Degrees of crankshaft rotation

DEF: Diesel Exhaust Fluid

DOC: Diesel Oxidation Catalyst

DOE: Department of Energy

ECU: Engine Control Unit

EGR: Exhaust Gas Recirculation

FEAD: Front engine accessory drive

FTP: Federal Test Procedure for transient engine test.

HRR: Heat Release Rate

MBF: Mass burn fraction

MGU: Motor Generator Unit

MY: Model Year

n_R: Number of crankshaft revolutions per cycle. 2 in this document; for a 4 stroke engine.

ORC: Organic Rankine Cycle

PCP: Peak Cylinder Pressure

PMEP: pumping mean effective pressure.

SOI: Start of Injection

VWP: Variable Water Pump

VGT: variable geometry Turbo

WHR: Waste Heat Recovery

The Analysis, Development and Calibration of Prototype Hardware in Effort to Improve Brake Thermal Efficiency and Real-World Fuel

Economy of the International Supertruck

Matthew Taylor

A THESIS SUBMITTED IN PARTIAL FUFFILLMENT OF THE REQUIREMENTS FOR THE DEGREE OF MASTER OF SCIENCE IN MANUFACTURING ENGINEERING TECHNOLOGY

MINNESOTA STATE UNIVERSITY, MANKATO

MANKATO, MINNESOTA

November 2023

ABSTRACT

The work performed for this project was in part of the effort of the Department of Energy Sponsored program called 'SuperTruck'. The entirety of the Supertruck program encompasses total vehicle re-design to achieve 80% freight efficiency improvement (over the 2009MY baseline production vehicle). However, the other main goal for the program is to achieve 50% engine brake thermal efficiency. The work outlined in this document describes the efforts performed on base engine and thus mainly contributing towards 50% BTE. Though ultimately reducing BSFC by increasing BTE contributes to both outcomes. The engine development data discussed in this paper was collected in a test cell at normal altitude and normal operating temperatures.   The bulk of the work that comprises this paper are in the research and development of new prototype and experimental hardware, and the calibration of such to maximize its performance yet still meet constraints. Constraints of the project are: the vehicle still needs to meet a 0.2 g/bhp-hr FTP-RMC combined tailpipe out NOx requirement, cylinder pressure limits for hardware durability, soot - and still maintain drivability - as the vehicle will be driven at what was determined a mean load of 68,000 pounds. A mule vehicle was built, referred to as 'T3', that encompassed some of the technologies and was demonstrated a year before the 'T4' truck was completed as to outline the team's progress on our path to the program's goals – some of that work is also discussed in this document. A MY2009 truck, used as a control, was also used to set baseline results, and will be referenced in this document.

Introduction

The CatalIST International Supertruck 1 vehicle in totality was a 5-year long project, beginning in preliminary stages in 2012 and the final report submitted in 2016. The project combined numerous people and teams with many areas of expertise. Numerous aspects of the vehicle were designed, built, and implemented specifically for this one-of-a-kind vehicle, and were the only of their kind.

Figure 1: The CatalIST International Supertruck Vehicle

Figure 2: T3 tractor

Weight Reduction:

The vehicle used numerous new features compared to a production vehicle to drop 2000lbs off the weight of the vehicle. The vehicle was a fully instrumented sleeper, even containing the mattress, and interior trim, so weight reduction was in other areas of the vehicle. Instead of standard steel leaf springs, composite leaf springs were made and implanted on the vehicle. Similarly, rather than standard glass windows, a special polycarbonate was specifically designed and produced for this vehicle. The biggest role of all might be the cab itself. It is a hand-made special carbon-fiber layup to maintain strength while reducing weight. Super-single rear tires were used instead of duals to reduce wheel and tire weight. The pie chart in **Fig. 3** shows the contribution to weight reduction of each of the components, in pounds.
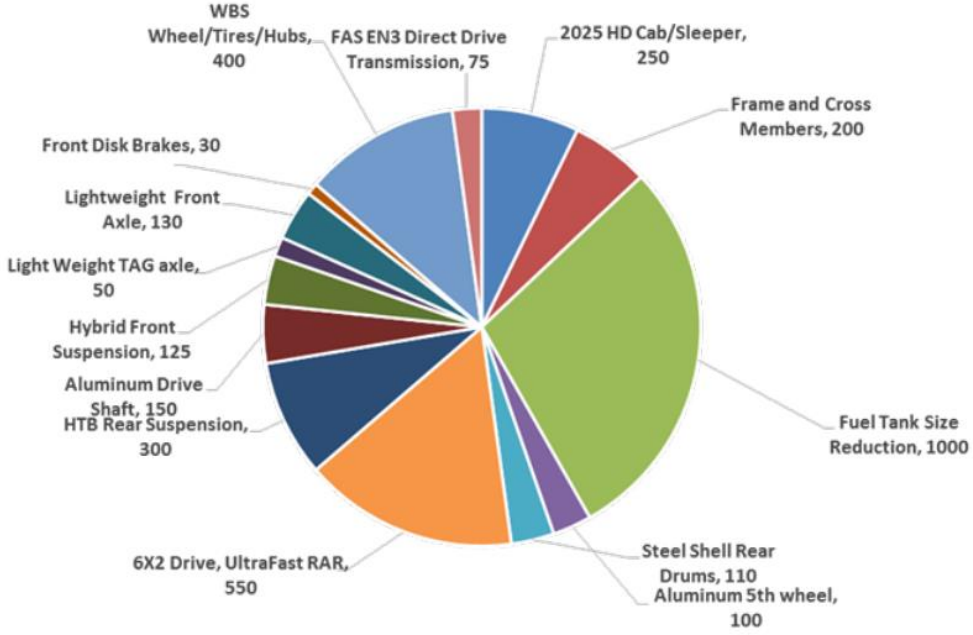
Figure 3: Weight reduction contribution by component set

From Navistar 2016 Q2 DOE report

Vehicle design and aerodynamic improvements:

The custom cab of the vehicle isn't just lighter, it is a design unique only to the CatalIST. It is about 5 inches wider at the rear, on either side compared to the standard ProStar Vehicle. Thus creating more of an "arrow" shape, and extensive work was done on a flow tunnel to determine the right lines and curves on the hood of the vehicle – not part of the scope of this paper. With the addition of bubbles on the forward end of the trailer that close in the gap between the cab and trailer, the wider body ensures air passes smoothly between the cab and trailer reducing eddy's, negative pressure, and thus, drag. Virtually everything was designed specifically for the Catalist vehicle; from the slope of the windshield, to the side skirts. This included the trailer. The boat-tail was extended on the tail end of the trailer, lengthening the path of the air passing behind it; allowing the air to join back together smoothly without

creating turbulence and thus negative pressures behind the vehicle – effectively pulling the vehicle backwards. All seen in **Fig. 4.** The gross vehicle dynamic equations, seen in **eq. 1**, explains how individual components like Aerodynamic (Faero), rolling resistance (Frf) and road grade (Fgra) subtract from the vehicle's available velocity over increments of time (slowing the vehicle down) thus requiring work (from the engine) to overcome these forces. Reducing the impact of each of these, has a cumulative effect on vehicle efficiency and therefore fuel derived work to move the vehicle down the road.

$$m_{eq} = \frac{dV}{dt} = Ftrac - Faero - Frf - Frr - Fgra$$

Equation 1: Overall Vehicle Dynamics

$$Faero = 0.5\rho airCdAf(V - Vair)^2$$

Equation 2: Aerodynamic (drag) Component

Vehicle dynamics equations from Basic Principles of Vehicle Dynamics

One of the biggest contributors to drag on the production vehicle are the exterior mirrors. The CatalIST replaces mirrors with cameras housed in aerodynamic mounts on the exterior of the vehicle (**Fig. 3**).   There are screens with multiple angles on the inside of the vehicle. Another unique feature of the CatalIST is the door handles. To complete a smooth body design, the latch mechanism is hidden inside a small pocket so as to create no air disturbances from protrusions from the vehicle. Another small piece of the cumulative structure are Timken Power Dense Fuel Efficient (PDFE) bearings; reducing the Frf component.

Figure 4: Rear View Camera

Vehicle Technology

One of the key contributors to the aerodynamics of the vehicle is the Hadley active ride height system – the working development and implementation of such is patented to members of the vehicle team.   The ride height system's module is added on to the vehicle CAN (Controller Area Network) network and receives vehicle information. As the vehicle reaches ~52 MPH (with some hysteresis calibrated into its operation) the front of the vehicle drops to where the front nose dam is merely 2 inches off the road. To put into perspective, the nose of a standard production tractor with an aero bumper will be ~11-13" off of the ground. While a tractor with a standard steel front bumper could 15" or more. The rear of the tractor doesn't drop quite as much as the front and back of the vehicle creating a rake around the trailer gap. This reduces turbulent air flow beneath the vehicle as well as cross the top of the trailer gap. Another feature this system can do is load bias the vehicle. It can reduce load from the drive axle to and to the tag axle. A tag axle is the axle behind the front differential. It is a hollow housing absent a differential which the second set of tires mount to. A very simplified equation for the purpose of a modest explanation of why load biasing is a unique tool that can be used to reduce Ftrac can be seen in **Eq. 3**.   If the adhesion coefficient (μ_t) and the weight on the drive tires (W) can be reduced, the vehicles Ftrac component is reduced.

$$\boldsymbol{Ftrac = \mu_t W}$$

Equation 3: Tractive Force Component

From Basic Principles of Vehicle Dynamics

The T4 vehicle is equipped with a 48V electric system, this is an integral structure to the vehicle. In addition to that, the entire roof on the trailer is a solar panel (**Fig. 4)**. This solar panel has been metered to be able to generate roughly ~5kW at a constant 100A @ 48V; when it's sunny conditions. The reason for this is to power all the electrification of the vehicle. The entire air conditioning system is electric and is ran off of a standalone system. There is no belt driven a/c compressor. Additionally, the vehicle is equipped with a 24V starter, a DC-DC converter and supercapacitor. This system is integrated in to an ISS (idle stop start) feature. The supercapacitor and 24V starter allows for greatly increased cranking from the starter resulting in much faster and smoother engine starting. The ISS feature allows the engine to reliably stop and re-start itself when idling at stop lights or stopped traffic. The 48V Li-Ion battery system and battery management system (BMS), also is the energy storage for the vehicle's micro hybrid system. The system uses a belt driven front engine accessory driven (FEAD) MGU and is capable of producing 15kW of power fed back to the engine through the belt. It can do this at 95% efficiency from battery to belt.   It also can switch from motoring, to generating when the BMS senses it needs more power. Moreover, it switches to an increased level of generating under braking events, thus being a form of regenerative braking and slowing down the vehicle.

Figure 5: Trailer Solar Panels

The engine cooling fan, like that on the mule vehicle, has 2 speeds and can draw upwards of 100 horsepower on highspeed. The Catalist vehicle utilizes a 3-speed engine cooling fan to add an even slower speed to minimize parasitic draw yet still provide heat transfer potential across the cooling pack. However, many provisions have been applied to prevent the fan from having to come on; at any speed. The vehicle is equipped with a "SmartCooling" system. For one, the engine uses a VWP to reduce engine belt drive parasitic losses, especially at the highway cruise point, which can give over 1% fuel economy improvement. Another facet of the system is increased coolant pressure which thereby increases the boiling temperature of the coolant. Having warmer coolant reduces the deltaT between the cylinder wall to the coolant, and thus, waste heat rejection absorbed by the engine coolant. This allows waste heat to be absorbed downstream, to be converted to work by the turbocharger, and even further downstream to the aftertreatment and the waste heat rejection system – rather than wasted to the coolant.

The most essential part of the system is Predictive Cruise Control (PCC) or SmartCruise. The predictive cruise control is constantly iterating and using GPS to look at the road and gradient ahead. If the system detects a grade ahead, it will signal to the VWP to increase pump speed. Increasing the pump speed before the added power demand, and thus fueling demand of the engine increases the heat rejection capacity of the coolant, thereby allowing the upcoming waste heat load to be absorbed into the coolant either reducing, or eliminating the need for the fan to come on. Furthermore, it can increase the vehicles speed, or even downshift into 9th gear so as to prevent a massive speed loss and engine lugging going up the hill. This creates a better driver feel, as well as fuel economy benefit.

An additional element of the engine is an improved efficiency, is a long stroke, single cylinder, clutch controlled air compressor. Tractor air compressors are mounted on the engine and driven by gear, creating a parasitic loss as it never stops rotating the crank and piston assembly.

During operation of this compressor, with the single cylinder, friction is decreased. With the longer stroke, it can still produce an adequate amount of air compression. While still being an engine-mounted gear driven pump, being clutch actuated, the pump only comes on when air pressure reaches a lower threshold. The pump rotating mass is then completely disengaged so that only the drive gear is spinning when it reaches an upper threshold, thereby decreasing parasitic loss - especially when at highway cruise and air consumption is a minimum. However, the most unique feature is that this air compressor is controlled by logic such that it is signaled to come on when in regenerative cycles, such as braking, or holding speed down hill. It couples that technology with over pressurizing what is a typical pressure of ~125 PSI, to 140PSI. To reduce its on-time during non-regenerative cycles.
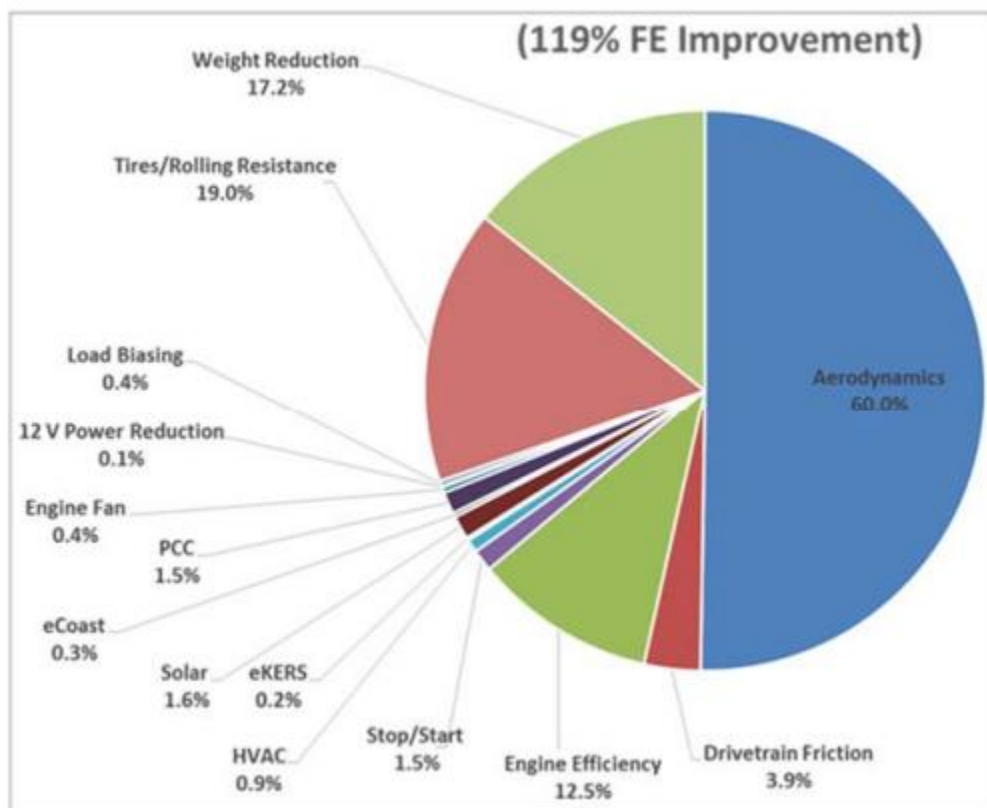
Figure 6: Efficiency improvement distribution from unique technology implementation on catalist Supertruck

Test Methodologies, Tools, and Instrumentation

The engine data presented in this paper are the actual results of an engine ran on a dynamometer in a test cell. The section of this paper details the tools and methodologies utilized to capture, post-process, and analyze the data presented.

- Exhaust Restriction Valve
- Intake Restriction Valve
- Emissions sampling tunnel
- Pressures and temperatures pylon
- Tunnel to laminar flow element
- Dynamometer, with strain gauge and load cell
- Charge amps to convert cyl. Press. transducer Raw signal
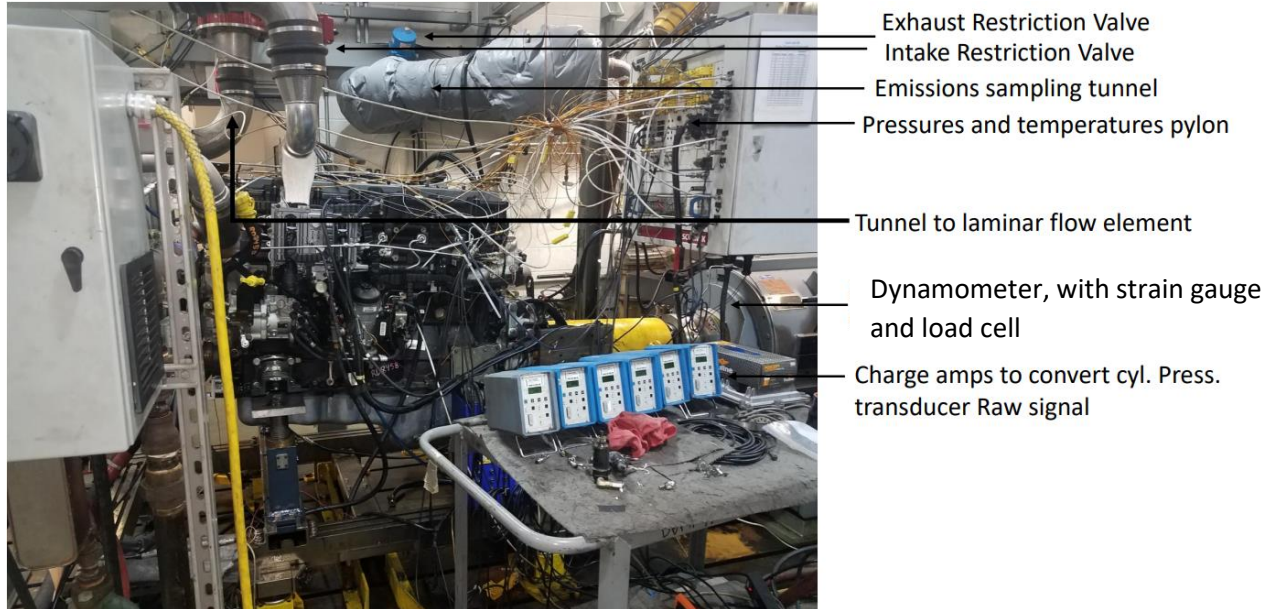
Figure 7: A fully instrumented test engine in the dynamometer room.

Test Cell:

The test cell is comprised of numerous essential hardware and tools to ensure accurate, repeatable, and reliable measurements. **Fig. 7** shows the engine in one of the test cells, and points out some of the tools and instruments discussed in this section.

Dynamometer: Eddy-current dynos are typically used in the facility, with some AC motoring dynos available. The eddy-current dyno was used to capture the engine speed and load desired of each test point.

Airflow: The test cell utilizes a laminar flow element to precisely measure the real-time air flow, utilized by the engine. The laminar flow element is essentially a fixed known orifice placed in-line of the induction air pipe, with a series of straight pipe on both the inlet and outlet. There are 2 pressure transducers, one on the inlet, and one on the outlet, generating a delta pressure measurement. The pressure transducers on each side of the laminar flow element are calibrated on a regular basis. Also on the intake piping is an intake restriction valve. This value is typically set at the pressure created by the intake system at rated speed and load. The pressure value is derived from restriction created by the air intake system to be used on the vehicle.

Fuel flow: While fuel columns are a common way to gather the fuel flow value of a test point, the data collected for this project utilized a ReSol fuel cart for quicker and more reliable fuel flow measurement.

Exhaust tunnel and emissions sample probe: While on certification level cells, a constant volume sample tunnel and an emissions bag are used, that is not necessary or practical for daily lab use. The exhaust setup for the experiments conducted for this paper is just comprised of a stack and vents to the atmosphere. There is an emissions sample probe near the outlet of the turbocharger. In the exhaust tunnel is an exhaust restriction valve. This valve is typically set to a pressure specified at the flow generated at rated speed and load. The pressure value is derived from the restriction created by the exhaust system to be used on the vehicle.

Emissions Bench: The Horiba 7000 series MEXA is used to measure the raw exhaust sample. The analyzer measures HC, CO, CO2, NOx, NO, THC, as well as intake C02 (EGR). The exhaust bench is shown in **Fig 8.** The screens on top show the live emissions measurement to the engineer and cell technician.

Figure 8: Horiba MEXA emissions measurement bench

Smokemeter: The AVL 415SE smokemeter is used to measure soot emissions concentrations of each test point.

Dyno controller: The dyno controller is used to set the desired transient cycle, or steady state speed and loads desired.

The pylon, data acquisition, and test cell PC: These 3 all work in conjunction to feed the raw signals coming from the engine instrumentation into discernable and usable data. The pylon contains the pressure transducers and thermocouple couplers that go to the data acquisition that filter and convert the signal, that then goes to the test cell PC which averages the measurements for the test points and then can store it so it accessible to the engineer.

Engine Instrumentation:

The engine is instrumented with approximately 15 temperature and 15 pressure sample ports. **Fig. 9** is an instrumentation request form utilized for one of the engines tested during this project. This shows all the sample areas instrumented on the test engine. In addition to the normal pressure transducers and thermocouples that go to the pylon. Turbo speed is measured with the Picoturn frequency box. The signal is then sent to an ETAS 441 frequency converter for processing, and that goes to the test cell PC to be included in the test cell data.

TEMPERATURES

X	LP CAC AIR (IN & OUT)
X	HP CAC AIR (IN & OUT)
X	INTAKE MANIFOLD
X	EXHAUST AT EACH PORT
X	HP TURBINE INLET (F&B)
X	LP TURBINE INLET
X	HP TURBINE OUTLET
X	LP COMPRESSOR INLET
X	HP COMPRESSOR OUTLET
	EGR VALVE INLET
X	EGR VALVE OUTLET
X	HT EGRC GAS IN (F & B)
X	HT EGRC GAS OUT (F & B)
X	LT EGRC GAS OUT (F & B)
X	LP CAC COOLANT (OUT)
X	HT EGR COOLANT (IN & OUT)
X	LT EGR COOLANT (IN & OUT)
X	FUEL SUPPLY / RETURN
X	COOLANT TEMP SHUTDOWN
X	OIL GALLERY
X	ENGINE COOLANT IN & OUT

PRESSURES

X	LP CAC AIR (IN & OUT)
X	HP CAC AIR (IN & OUT)
X	INTAKE MANIFOLD
X	HP TURBINE INLET (F&B)
X	LP TURBINE INLET
X	HP TURBINE OUTLET
X	LP COMPRESSOR INLET
X	HP COMPRESSOR OUTLET
X	EGR VALVE INLET
X	EGR VALVE OUTLET
X	HT EGRC GAS IN (F & B)
X	HT EGRC GAS OUT (F & B)
X	LT EGRC GAS OUT (F & B)
	HT EGR COOLANT (IN)
X	FUEL SUPPLY / RETURN
X	CRANKCASE
X	OIL GALLERY
X	CYLINDER PRESSURE (6)

SPECIAL REQUIREMENTS

Intake manifold CO_2 measurement (2)

Cylinder pressure/IndiCom/Crankshaft encoder

Turbo speed for HP turbochargers

MISCELLANEOUS

OIL SAMPLE

COOLANT SAMPLE

Figure 9: Engine Instrumentation List

Cylinder pressure transducer: One of the most important pieces of instrumentation is the cylinder pressure transducer. The cylinder head is machined to accept the Kistler 6125C pressure transducer that has an accurate range up to 4350 PSI. In addition to the pressure pick-up, there are a few pieces of supporting hardware, as well as software. A pressure transducer is shown in **fig. 10.**

Cylinder pressure charge amplifer: The cylinder pressure pick-ups are calibrated to a value of picoCoulumb (pC) per PSI, or pC/PSI. The Kistler cylinder pressure charge amplifier, takes the raw signal from the pressure pick-up, which is in pC and convert it to PSI/Voltage, such that the transfer function of the Indicom PC can translate into PSI.

AVL Indicom hub: The encoder hub is used in conjunction with the pressure pick-up to reference the cylinder pressure waveform to crank angle. Both of the signals from these components are then sent to a separate PC which runs the software that processes these signals as well as providing a live reading of the measurement. The Indicom hub, and supporting hardware, is shown in **fig. 11**.
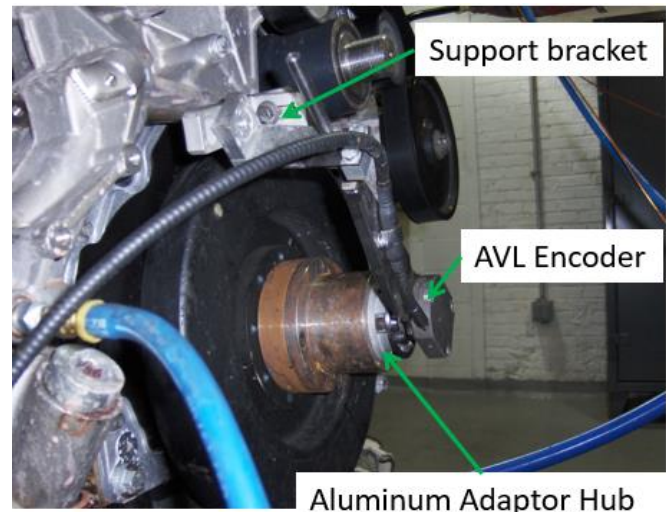
Figure 10 and 11: A calibrated pressure transducer before installation (10) and the AVL encoder installed on a test engine (11)

Indicom: Indicom is software for recording and post-processing of cylinder pressure measurements.   This program runs on a separate PC in the test cell, but its results are built in the combined data file produced by the dyno cell. The engineer can view the cylinder pressure wave live in the test cell, which can provide instant feedback to the test point's effect on combustion. But that is only 1 feature of the software. When the dyno operator takes a measurement point, it also takes a recording on Indicom, producing an "I" file. This file can be analyzed in a separate program, called Concerto. Should the engineer want to integrate heat release rate, examine anomalies in the combustion data, build the P-V diagram, or many other features. The most useful feature, relevant to the work presented in this paper, is the following: BMEP, FMEP, IMEP, and the significant measures of mass burn fraction (i.e. 5%, 10%, 50%, 90%, 10%-90%, and 50%-90%) are part of the data post-processing of the dyno cell, and
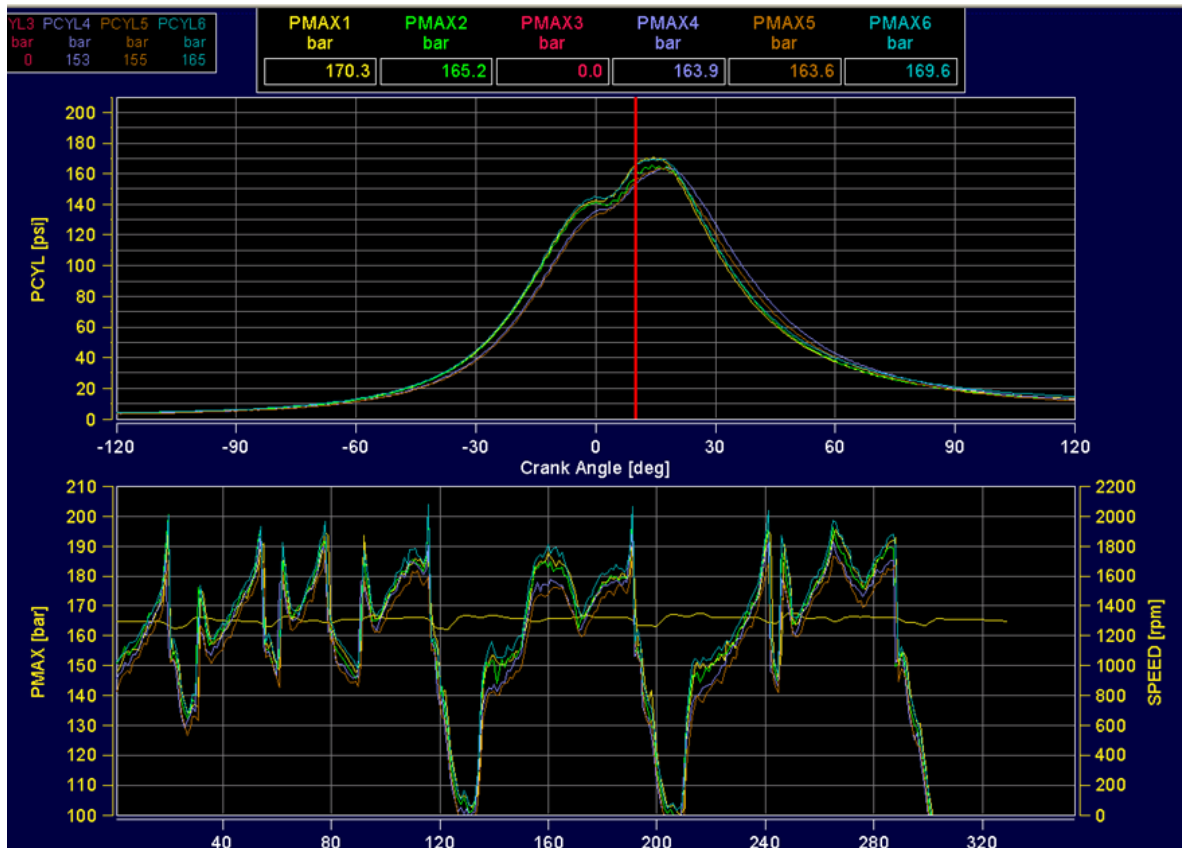
Figure 12: The screen of the Indicom PC in the test cell

merged into each of the datasets from each test conducted. Thus, it is extremely easy to analyze and plot along with the other data captured from the cell, like BSFC for example. This is extremely useful as it allows the engineer to examine the results from the calibration setpoint's effects on the heat release rate and it's effect on BSFC and BTE. For some of the work presented in this paper, the analysis of these types of plots are discussed. Refer to **fig. 12** to see what the Indicom computer displays while the engine runs on the dyno. Notice it shows as many cylinders as are instrumented, on top of each other. Meaning, the software aligns all cylinders relative to the same axis, even though they are firing at different times. Likewise, it also shows the cylinder pressure traces, in an engine speed domain, over time of the test.

Calibration Software: The software tool most critical to the work described in this paper is that used to calibrate the engine. ETAS INCA is a tool that interfaces with the ECU (engine - or electronic - control unit) and can control the engine by emulating the RAM memory. Meaning, the engine will run off the parameter setpoints selected by the engineer instead of those that are written, or "flashed", on to the ECU's hard memory. For the ECU or INCA to know what the parameters that make up the control systems strategy are for a particular variant of engine, a software file, called an A2L is needed. There are thousands of variables contained in that A2L file. The .HEX file, or the calibration file, is what is flashed into the ECU. The .HEX file holds the calibrated values of each of those thousands of labels for the engine to continuously and rapidly reference, for seamless operation.

For the tests conducted with different pieces of hardware (like an injector set, or turbocharger, etc.) the engineer, would determine what parameter of the calibration to manually set, and to what values they should be set. A test request is submitted to the test cell technician, containing the test matrix of engine speed and load and the parameters and their values they should run to yield a useful dataset. Then, the calibration engineer, would use INCA to build new calibration maps based upon the results of the tests. I would then flash these changes into the ECU and we would run confirmation tests, like a complete or reduced engine map, to validate the newly built calibration. The analysis of the hardware tests and presentation of the results of the calibration that was developed for the Supertruck, are to be discussed in this paper.

Data Quality:

It has been mentioned in this section that each piece of instrumentation receives frequent calibrations individually. Having known-good and documented instruments is essential to producing reliable and repeatable data. Furthermore, if the instruments can be trusted, it makes it easier to notice when a piece of equipment, measurement device, or hardware fails. Every effort is made to ensure the test being conducted in the cell will produce accurate and useful results. As such, every day, a checkpoint is ran on the engine; typically at rated speed and load. This is because the restrictions are usually set at rated, as intake, fuel and exhaust flows are the highest. The settings for the daily checkpoint can be seen in **Fig 13.** One of the primary tell-tale parameters that highlights a potential data quality issue is called carbon balance. This is calculated figure, made up of the sum of carbon going into the engine, as measured by the airflow and fuel flow meters, compared to the carbon coming out of the engine, as measured by the emissions bench. In-house, we say if your check point falls within +/- 3% carbon balance error, you should have a reliable test. **Fig. 14** presents a few weeks' worth of checkpoints on the primary calibration development engine. It can be seen that the points continue to fall within that +/- 3% margin. Should carbon balance be low negative value, it would be assumed there is an exhaust leak, meaning, carbon is being lost before it can be measured. Should it be high, there may be air leak or fuel leak after the ReSol cart as more carbon is measured out than what was measured coming in. But, other metrics, like air flow, fuel flow, even torque, are also examined to be sure there aren't other mechanical issues. Additionally, when running the checkpoint, the cell technician will adjust the intake and exhaust restriction valves as needed, to ensure every aspect of the test can be reliably repeated, even if it was days or weeks prior.   All data presented in this paper received the same scrutiny of data quality checks and for this reason will be presented as accurate and trusted results.

Settings at Daily Checkpoint (DCP) Speed/Torque: 1700 RPM/1467 ft-lb				
Temperature:			Pressure:	
Fuel Temp = 100 +/- 1 °F			Intake restriction controlled to 13.0 +/- 0.5 inH20	
Compresssor air inlet temperature set to 77 +/-2 °F			Exhaust restriction set to 6.2 +/- inHg	
HP CAC out temp: 100 +/- 2°F			- Exhaust restriction set at "HP Turbine Outlet"	
Engine out coolant temp = 208 °F			HP CAC ΔP to 4.0 +/- inHg	
Fuel Injection System:			Control Valve Position:	
Rail pressure = 2500 bar			EGBP = 66in hg	
Main timing (SOI) = 11 bTDC			By adjusting EGRv target NOx = 450 ppm	
InjCrv_stInjCharActVal = 1010			*Set VWP to 5000 RP (or 0% duty cycle, 1:1	
Post separation timing = -950us			with pully)*	
Post quantity = 10 mg/hub				

Figure 13: Daily Checkpoint settings for the calibration engine used in to present the data in this paper.
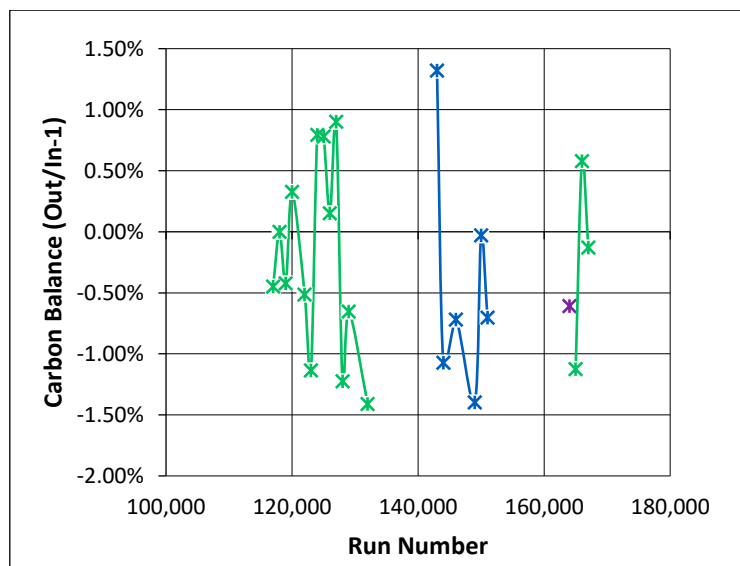
Figure 14: Actual carbon balance tracking from daily checkpoints ran on the calibration development engine. The results of which are presented in this paper.

Chapter 1 – Downspeeding, Engine Dynamics, and Calibration Implications on HW and Federal Cycles

The calibration effort described in this document focuses around three main areas, that are reflected on 3 main pillars of the areas of concentration to achieve the project objective of 50% BTE. From the waterfall in **Fig. 15**, 3 main contributors on the path to 50% BTE are downspeeding (the lug curve), gas flow optimization, and advanced combustion. The focus of this chapter is to explain the effects of downspeeding and how the T3 and T4 vehicles were modified to accept the new operation range of the engine.

Path to 50% BTE:
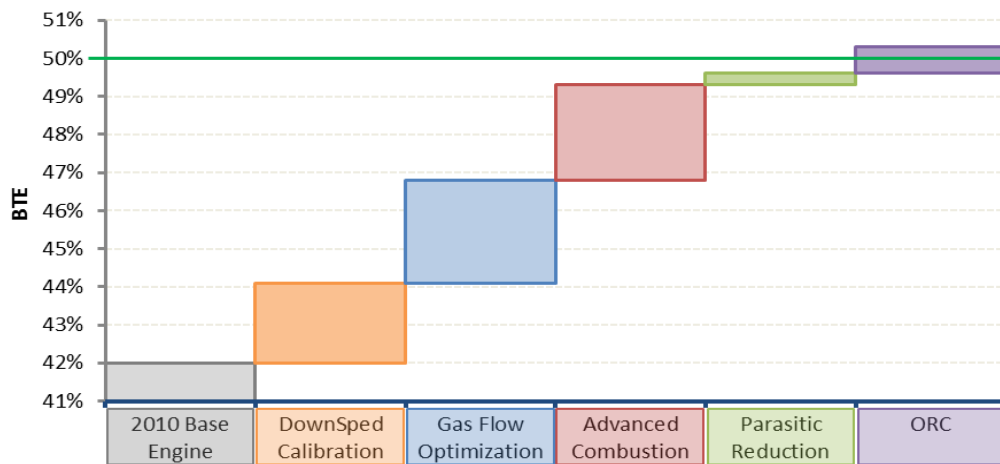
Figure 15: Waterfall of actual demonstrated BTE with selected technologies

From Navistar 2016 Q2 DOE report

Fig. 16 illustrates the difference in the lug curve from the baseline 2009MY engine, and the new lug curve for the Supertruck engine. Peak torque goes from 1691 ft-lb up to 1850 ft-lb. In addition, peak torque starts at just 900 RPM and holds to 1100 RPM.   The peak horsepower, of 400, is achieved at just 1200 RPM, and peak HP is held through 1600 RPM. Quite a difference from the 2009MY 475HP, 1691 ft-lb lug curve. Notice the difference of area under the curve on the left side, or slower engine speed side, of the map. This maximizes the higher BMEP points of the engine. The work done over the 4 cycles of a diesel engine can be defined rather simply by **eq. 4**.

$$W = \oint P dV$$

Equation 4: The integral formula for work done by an ICE

From Internal Combustion Engine Fundamentals

Or, in terms of the First Law of Thermodynamics by **eq. 5.**, with respect to the crank angle domain of 4 the cycles, or 720 degrees of crankshaft rotation. Which also accounts for the

work done by the system, during compression and pumping. Stating that the total work done over all the degrees of crankshaft revolutions, equals the work done by the system, dQ, minus the work done to the system, dW.

$$\frac{dU}{d\theta} = \frac{dQ}{d\theta} - \frac{dW}{d\theta}$$

Equation 5: Work done on a diesel cycle with respect to crank angle

Simplified from Internal Combustion Engine Fundamentals
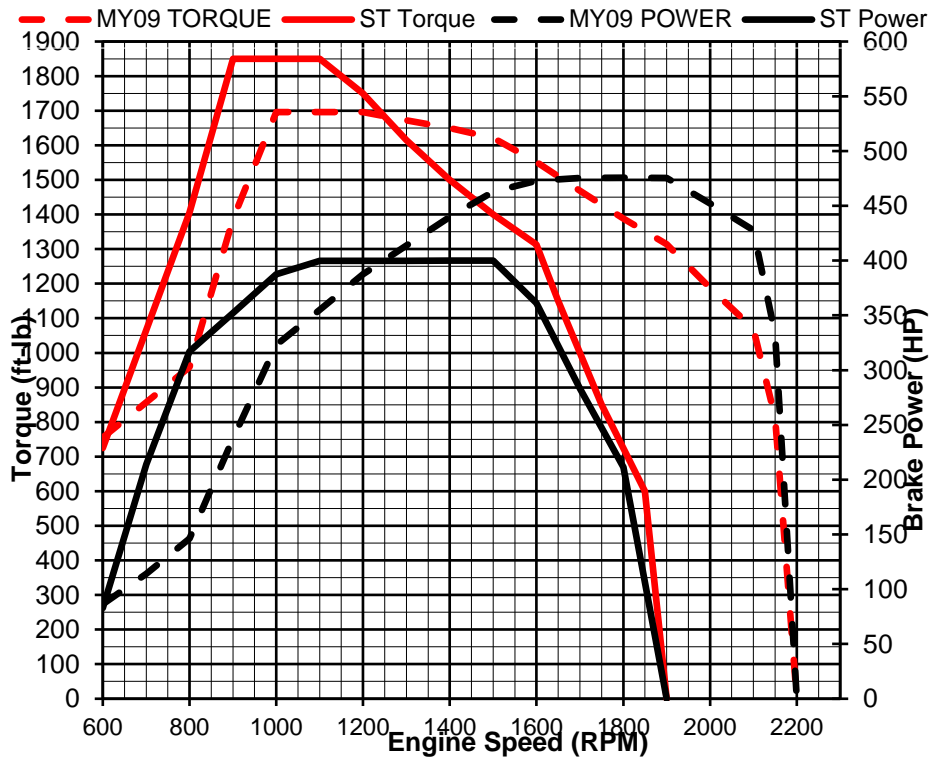
Figure 16: MY2009 Lug Curve vs Supertruck LugCurve

This equation shows its relationship to P-V diagram, illustrated in **Fig. 17**. The area confined by the 0-1-2, points, is the work done do the system, and the area confined by the 1-2-3-4 points, is the work done by the system. The mathematically derived value, as a function of torque, used to quantify the work done in the P-V domain, with respect to engine size is called BMEP. The equation for BMEP in units of PSI, is shown in **Eq 6.**.

$$\text{mep(lb/in}^2) = \frac{75.4 n_R T(\text{lbf} \cdot \text{ft})}{V_d(\text{in}^3)}$$

Equation 6: Brake Mean Effective Pressure

From Internal Combustion Engine Fundamentals
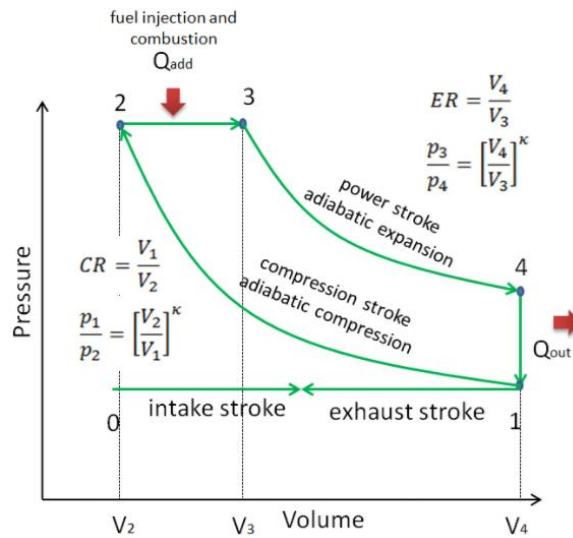
Figure 17: Diesel Cycle P-V Diagram (constant pressure - isobaric)

From nuclear-power.net

Referring back to **Fig 16.**, the new peak torque points of the Supertruck lug curve will have higher BMEP than the peak torque of the MY2009. Additionally, moving the lug curve to lower speeds now gives more points with higher BMEP, relative to the 2009MY baseline. The effect of BMEP from engine speed, and where the Supertruck engine is optimized to operate can be shown in **Fig. 18.**

With 3 clusters of points at engine speeds 1000, 1500, and 1700 RPM taken from the engine map, notice how the BMEP moves upward as the speed trends downward. On the left of the figure, depicting the MY09 lugcurve area, highlights where the Supertruck engine is optimized to operate due to this reaction.
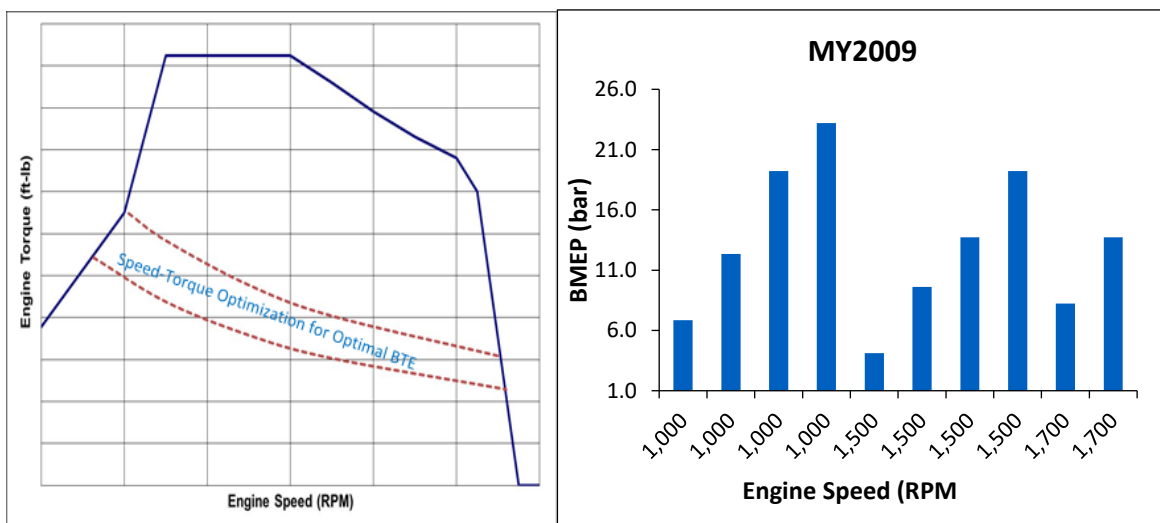
Figure 18: BMEP trend from MY2009 engine map and depiction of where this map is to be optimized for improved BSFC.

The BSFC benefit from downspeeding, from the increased BMEP, is illustrated in **Fig 19.** If keeping the same power, in this case 150HP and 180HP, and move the speed at which this power is reached, increasingly lower; BSFC will also continue to decrease. However, it should be noted that there does appear there is an inflection point around the end point of 900 RPM, and going any further would not yield any benefit to BSFC.

Optimized BSFC (across the constant power-lines)
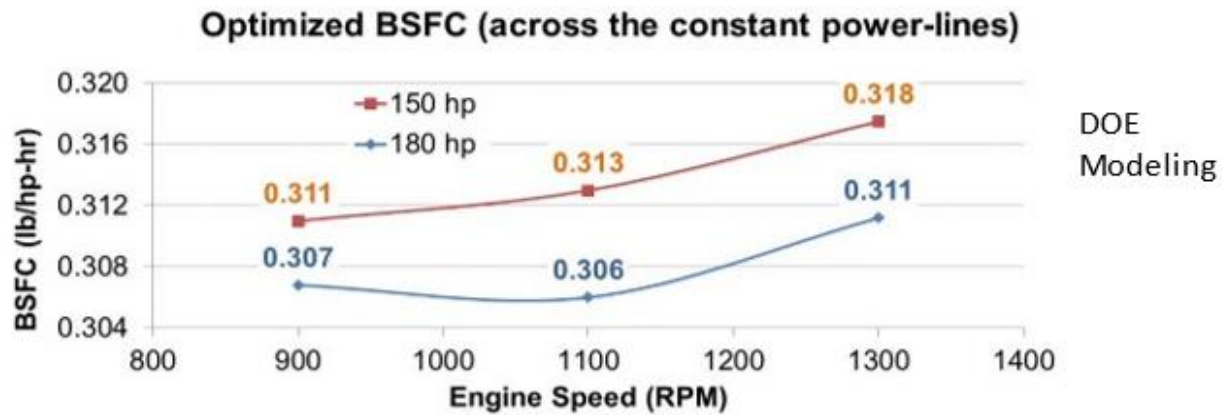
Figure 19: Effect of Downspeeding on BSFC

Courtesy of Navistar Inc.

BSFC can be lower at lower engine speeds where torque is high for the following reason: reduced pumping losses, reduced friction losses, better efficient air flow dynamics and and fuel mixture. Based upon Eq. 5 and Fig. 17, more work is done by the system and less work is done to the system. Thermodynamically, more work per cycle, per unit displacement. While all of this is ideal from a theoretical BTE standpoint, this only tells part of the story for the purposes of Supertruck. If a vehicle can be improved such that it takes less power to move it, now less torque is also required in addition to less speed (i.e. horsepower). While the reduction of fueling, as a whole, is a function of the two goals of Supertruck; 50% BTE and 80% freight efficiency improvement, they can also be slightly exclusive from one another. Meaning, if the vehicle is improved such that less power is needed to move (at 65 MPH) at a lower engine speed, then the benefit to the freight efficiency improvement may not correlate to peak BTE of the engine. That point can be explained in the following section.

In order to effectively utilize the lower speed operation, the T4 truck is equipped with an only-of-its-kind differential ratio of 1.91:1 which mates to 10-speed Eaton automated manual transmission (AMT) with a direct drive (1:1). The control truck utilizes a 3.21:1 axle ratio, but has a 10spd overdrive transmission. The difference in these configurations moves the 65mph cruise point from roughly 1300 RPM 50% load, or B50, down to roughly 1000 RPM 50% load point, or, A50. Effectively utilizing the left side of the map, shown in Fig. 16 . With the lower engine speed should come a lower fuel consumption. To evaluate this effect, a comparison test was performed on the T3 vehicle vs the control vehicle. In 2015, the T3 vehicle was presented to the DoE to as a demonstration of progress on the project and the technologies used to get

there. The demonstration took place at the Navistar Proving Grounds (NPG) in New Carlisle, IN. At NPG, there is a 2-mile oval test track in which the vehicles can run the same repeatable test without variables like traffic or road hazards. The driveshaft was instrumented with a Binsfeld torque meter, and real shaft torque was measured; so horsepower could be calculated. Additionally, utilizing ECU maps, real time fuel flow could be calculated to compare the difference in fueling between the 2009MY baseline truck and the T3 Supertruck mule vehicle. The vehicles ran the test at the same time and the data presented in **Fig. 20a and b** are from the recorded data of that test. In **Fig. 20a,** the green line shows the engine speed of the T3 truck, with the 1.91:1 gear ratio and 1:1 10th gear, or top gear, at 65 MPH. The blue line shows the engine speed of the control vehicle, with the 3.21:1 gear ratio and overdrive 10th gear, or top gear, at 65 MPH. The red line shows the effect of shifting down to a 1:1 ratio in 9th gear, of the control vehicle. Notice the engine speed lands at ~1750RPM at a 1:1 transmission ratio. This highlights the effects of the numerically low rear axle ratio on engine speed.
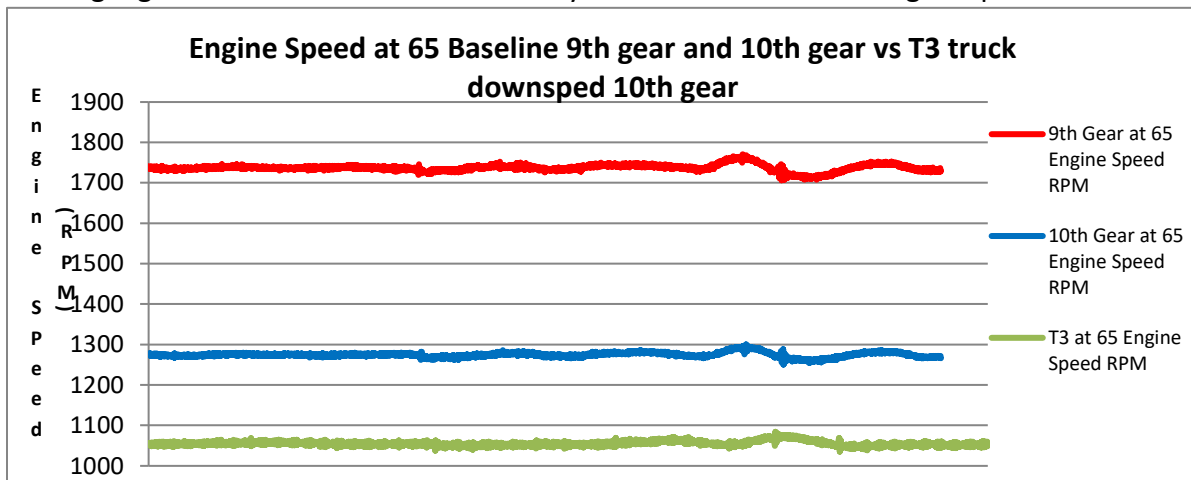
Figure 20a: Effect of downsped vehicle gearing package on engine speed

The resulting effect on the horsepower of the new speed of the engine at highway cruise is illustrated in **Fig. 20b.** The blue line shows the horsepower trace of the control vehicle. Averaging the data from this cycle shows ~207HP to run the truck at 65MPH. The green line shows the horsepower trace of the T3 truck. Averaging the data from the cycle shows ~150HP to run the truck at 65MPH. The benefits of the technology improvements of the T3 truck being demonstrated, that are implemented in the final T4 Supertruck, can be quantified. The Hadley ride height adjustment system and trailer skirts, lowering the Coeffecient of Drag-Cd, and the numerically low axle gear, 1:1 10th gear ratio, and the low friction wheel bearings lower the rolling resistance-Frr combine to make less drag and thus, less power required for sustained propulsion at 65 MPH. The differences in fueling can be derived from the ECU fueling, engine speed, and driveshaft torque measurements. While it should be noted that ECU calculated fueling values are not nearly as accurate as a separate stand-alone fuel flow meter, since the methodology is the same between each truck the comparisons can still be drawn from the data.
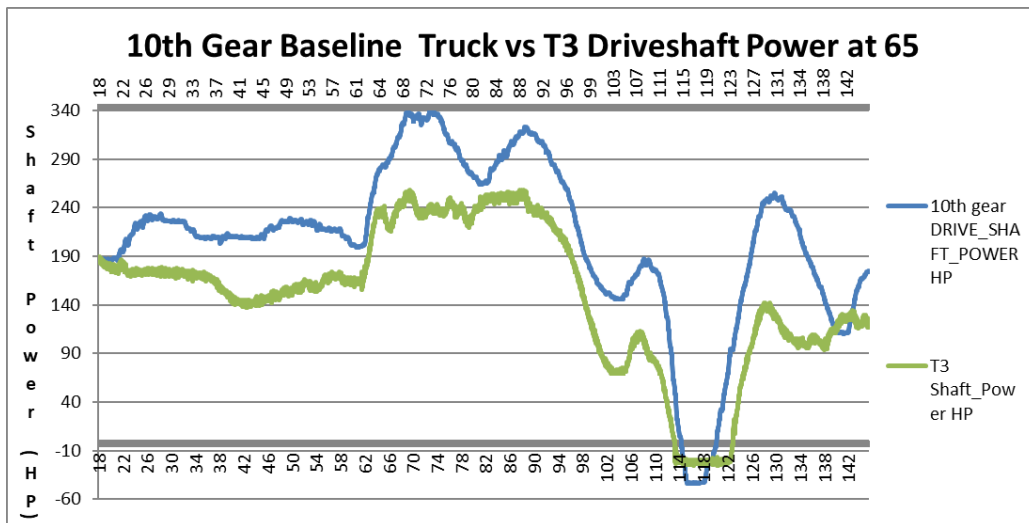
Figure 20b: Shaft HP difference of loaded vehicle – T3 truck vs 2009MY baseline

Deriving the engine torque can be back-calculated from the horsepower utilizing Eq. 7.

$$HP = \frac{TxRPM}{5252}$$

Equation 7: Horsepower from torque (ft-lb) and engine speed (RPM)

Engineering Fundamentals of the Internal Combustion Engine

Deriving the BMEP can then be performed by utilizing Eq. 6. BSFC, in unit lb/hp-hr can be calculated by using **Eq. 8**. Utilizing for #2 diesel pumped from the on-site fuel island for this demonstration, where the constant 7.1 is the weight of fuel per gallon, in pounds.

$$\text{BSFC} = \frac{Fuel\ flow\left(\frac{g}{h}\right)*7.1}{Horsepower}$$

Equation 8: BSFC from the measured fuel flow and horsepower

From Internal Combustion Engine Fundamentals

Deriving BTE can be derived from **Eq. 9**. Heywood refers to thermal efficiency as "fuel conversion efficiency"[1]. The lower heating value is utilized for Q_{HV}, of 18521 BTU/lb

$$BTE = \frac{2545}{BSFC*Q_{HV}}$$

Equation 9: Brake Thermal Efficiency

From Internal Combustion Engine Fundamentals

Then the average miles per gallon can be calculated taking the average vehicle speed of 65 mph divided by the averaged measured fuel flow of gallons/hour. The results of these calculations are shown in **Fig. 21.** Since the T3 vehicle's improved efficiency allows for such lower

horsepower to sustain it at 65 MPH, the average torque is decreased, even at the lower engine speed.

Control Average HP		224
T3 Average HP		162
Control Average g/h		10.9
T3 Average g/h		7.48
Control Average Speed		1274
T3 Average Speed		1055
Control Average Torque		922
T3 Average Torque		806
Control Average BMEP		183
T3 Average BMEP		161
Control Average BSFC		0.3462
T3 Average BSFC		0.3278
Control Average BTE		37%
T3 Average BTE		42%
Control-Caclulated MPG		6.0
T3-Calculated MPG		8.7

Figure 21: Measured effect on vehicle technology and architecture, and engine down-speeding on fuel economy.

As a result, the BMEP is actually lower than that of the control, but still showing major improvements in fuel economy - showcasing the benefit of the vehicle improvements to rolling resistance and drag.

At the time of this test 2 vital hardware selections have not been finalized. The turbo charger and the cylinder head are better optimized on the T4 vehicle. Additionally, hardware additions like that of the variable water pump, are not included on this mule engine. But this demonstration test gives good insight on how the vehicle and engine work together to achieve the goals of Supertruck.   Adding 8% to the driveshaft horsepower values to estimate the losses through the transmission yields an estimated ~224 HP from the control vehicle, and ~162 HP from the T3 vehicle to, as shown in Fig. 21. Then utilizing Eq. 8 and 9, it is possible to calculate the specific fuel consumption from the engine. The results show over 5% improvement in BSFC, which directly correlates to the 5% improvement in BTE; proving the beneficial relationship to downspeeding the lug curve and BTE improvement.

There are affects from down-speeding that need to be considered when making final hardware selections and can also present challenges when making the calibration to meet the constraints from emissions and hardware limits. The shift in lug curve also means a shift on the engine speeds and loads for the USEPA Heavy-Duty Supplemental Emissions Test (SET) 13 Mode steady state test. **Fig. 22** compares the difference between the speed and loads points for the 2009MY

			Supertruck		2009MY		NOx weight factor
	Speed	% torque	Speed	Torque	Speed	Torque	
mode 1	Idle	0	700	41	600	41	0.1%
mode 2	A	100	1023	1850	1205	1674	12.6%
mode 3	B	50	1267	829	1510	807	9.3%
mode 4	B	75	1267	1243	1510	1210	14.0%
mode 5	A	50	1023	925	1205	858	3.9%
mode 6	A	75	1023	1388	1205	1288	5.9%
mode 7	A	25	1023	463	1205	430	2.0%
mode 8	B	100	1267	1658	1510	1586	16.8%
mode 9	B	25	1267	414	1510	403	4.7%
mode 10	C	100	1511	1391	1810	1355	15.8%
mode 11	C	25	1511	348	1810	347	2.5%
mode 12	C	75	1511	1043	1810	1041	7.4%
mode 13	C	50	1511	695	1810	694	4.9%

Figure 22: 13M speed and load comparison with NOx weighting factor

engine and the Supertruck engine. Among performance concerns, as mentioned, the engine still needs to meet the 0.2 g/bhp-hr tailpipe NOx requirement. To achieve this, the engine is still equipped with a selective catalyst reduction (SCR) system which injects (doses) urea in the exhaust stream and passes the gas/urea mixture across a catalyst, and converts the NOx to N_2 and H_2O. As engine speed is lowered, NOx conversion becomes more difficult. In order to meet the tailpipe NOx reduction, NOx conversion efficiency will need to be upwards of 98% or higher. For that to happen three things are required, temperature, flow, and urea. If flow too low relative to urea, the urea cannot remain suspended in the mixture, drops out and crystalizes. If temperature too low, the catalyst brick cannot convert effectively, and if too low, urea cannot be injected at all rendering the SCR useless. Thus, engine inefficiencies are good for SCR but antithetical to the goal of Supertruck. Coupled with the SCR, an EGR system is also used to lower engine out NOx, going to the SCR system. As engine efficiencies improve, and pumping losses are decreased, the ability to flow (drive) EGR is also decreased. The engine requires dP, or positive back-to-boost pressure to effectively flow EGR. This again is counterproductive to the goal. Along with pumping loss reduction, downspeeding poses a challenge to achieving ample back to boost. As engine speed is lower airflow is lower, as airflow is lower, back to boost is also lower. Taking note of the NOx weighting factors in Fig. 22. C100 NOx is the most heavily weighted point in the cycle. With the engine speed 300 RPM lower on the Supertruck lug curve, selecting the best hardware, and building the calibration to improve BTE, but also drive EGR will be balance. This is presented here to explain there are nuances, considerations, and cost/benefit analyses that have to be made throughout the hardware selection, and calibration process which may hurt BTE, or pose risks to hardware. For example, the turbocharger to be selected will see an increase its combined efficiency (compressor+turbine) to improve engine BTE. As a turbine's efficiency improves, it is able to convert the waste exhaust energy more effectively, thereby lowering the turbine out temperature. Lower turbine out temperatures are bad for SCR NOx conversion efficiency. More efficient turbocharger wheels lower engine dP, which is bad for back-to-boost. This is discussed more in chapter 3.

Chapter 2 – Combustion system and Bowl-Nozzle Configuration

Referring to chapter 1, gas flow optimization is a main pillar on the path to 50% BTE. The combustion design is completely re-engineered from the 2009MY. Although discussed more in chapter 3 with the turbocharger selection, a major driver of the increase in BTE for the Supertruck engine is air:fuel ratio (AFR). For AFR to be increased and to be effective the cylinder head, piston, fuel injector, and turbocharger will all need to be selected to work in conjunction with one another. Immense engineering effort and resources went into the piston bowl design. The ideal compression ratio for the hardware selected, was chosen to by 20.5:1; a marked increase from the 2009MY compression ratio of 17:1. Increasing compression ratios increases thermal efficiency.
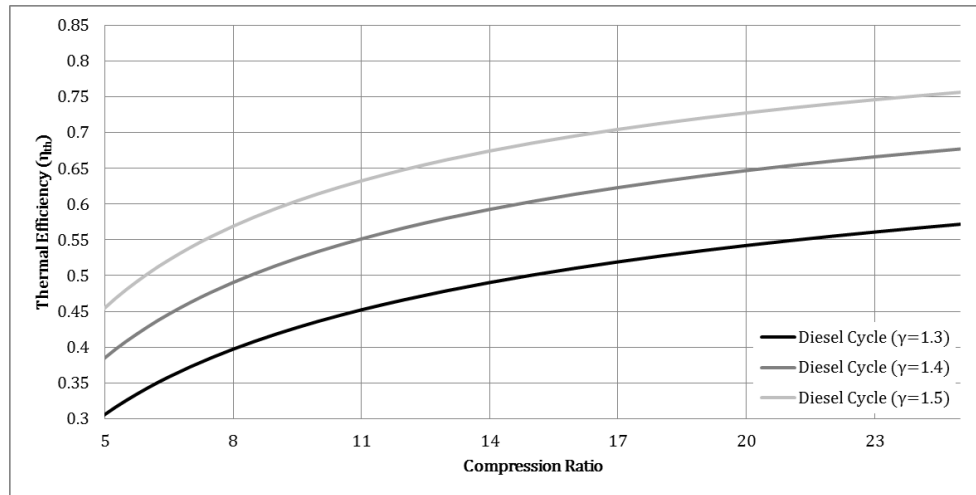
Figure 23: Thermal efficiency vs engine compression ratio

From SAE Technical Paper 2018-01-0237

This can be illustrated by **Fig. 23.** Referencing the graph, a compression ratio of 20.5 should be capable of an indicated thermal efficiency of ~60% when using a gamma value (k-value) of 1.35. The explanation of this can be thermodynamically derived using **Eq. 12**. Where *r* is compression ratio shown in **Eq. 10.** r_c is cuttoff ratio, shown in **Eq. 11.** Gamma is the specific heat ratio of constant pressure (C_P) divided by constant volume (C_v).

Compression ratio = V1/V2

Cutoff ratio =V3/V2

Equation 10: Compression Ratio and **Equation 11:** Cutoff Ratio

$$\eta_{th} = 1 - \frac{r^{1-\gamma}(r_c^{\gamma}-1)}{\gamma(r_c-1)}$$

Equation 12: Diesel Cycle Thermal Efficiency

From www.nuclear-power.com

For equations 10 and 11, refer back to fig. 17 to review V1, V2, V3, and V4 . Based upon the chart shown in fig. 23, it would seem intuitive that a higher compression ratio would have yielded even better thermal efficiency.   However, it should also be noted that even though thermal efficiency seems to keep improving as compression ratio increases so does engine pumping. Continuous increases in compression reaches a point of diminished returns. Compression ratio will eventually decrease BTE as the contribution to engine pumping (or negative work) surpasses its benefit in thermal efficiency gains to BTE[9]. The effect of increasing compression ratios can be shown in **Fig. 24.** Three development pistons were run on the same engine, C4-18.5:1, C5;19.5:1, and NS4-20.5:1. There is an upward trend in BTE as the compression ratio is increased.   Additionally, there is a direct correlation to peak cylinder pressure with each increment in compression ratio. This increased firing pressure is what eventually has the negative impact on pumping as compression continues to be increased.
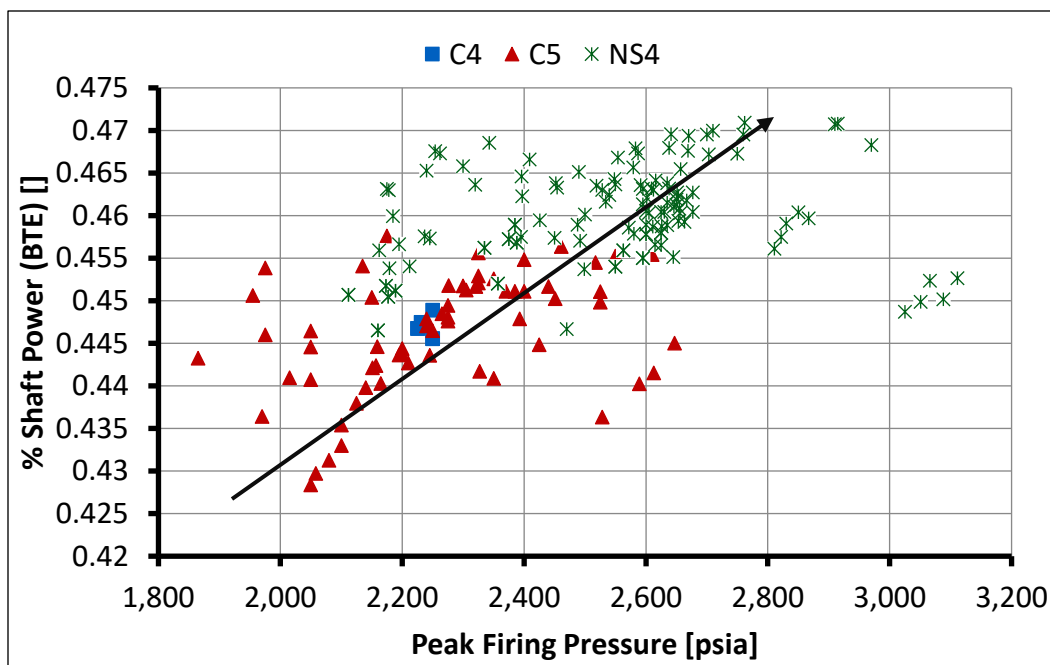
Figure 24: BTE vs peak cylinder pressure of 3 pistons of increasing compression ratios

Courtesy of Navistar Inc.

However, the higher cylinder pressure can be utilized to promote faster combustion, in so doing increasing the heat release rate (HRR). Which, the combustion scheme of Supertruck is aiming to achieve.   A further explanation of eq. 11, will explain the engineering behind combustion system design. Cutoff ratio is the volume displaced during the heat addition, i.e., the combustion event. If the ratio is 1, meaning combustion happens instantaneously at TDC, thermal efficiency is 100%. So, increasing HRR closer and closer to TDC increases thermal efficiency. Trapping more air in the cylinder with a high AFR, shortening injection time with high pressure/high flow fuel injectors, and increasing *r* will all work together to increase the HRR and thermal efficiency. In efforts to reduce restrictions to airflow and maximize AFR, swirl is reduced, and a quiescent combustion approach is used. To reduce the swirl the intake port

was opened, volume increased, and wider valve seat and larger intake valve are used, which increase the flow capability of the cylinder head. To match with this combustion scheme, the NS4, or no swirl, iteration 4, bowl is chosen. The difference in bowl profile of the 17:1 piston from the 2009MY, and the NS4 20.5:1 from Supertruck is shown in **Fig. 25**. Notice how much wider and shallower the bowl is. This bowl design will rely on the highly atomized fuel from the high injection pressure coupled with higher compression pressure to achieve rapid and thorough mixing of the fuel and combustion air. The wider bowl is to promote combustion closer to TDC in effort to increase HRR.   With higher injector pressures, fuel injector energization time is reduced as fuel can enter the cylinder faster. As a result, it is presumed this piston bowl benefits from fuel being shot wider for a shorter duration, rather than deeper in the cylinder for a longer duration.
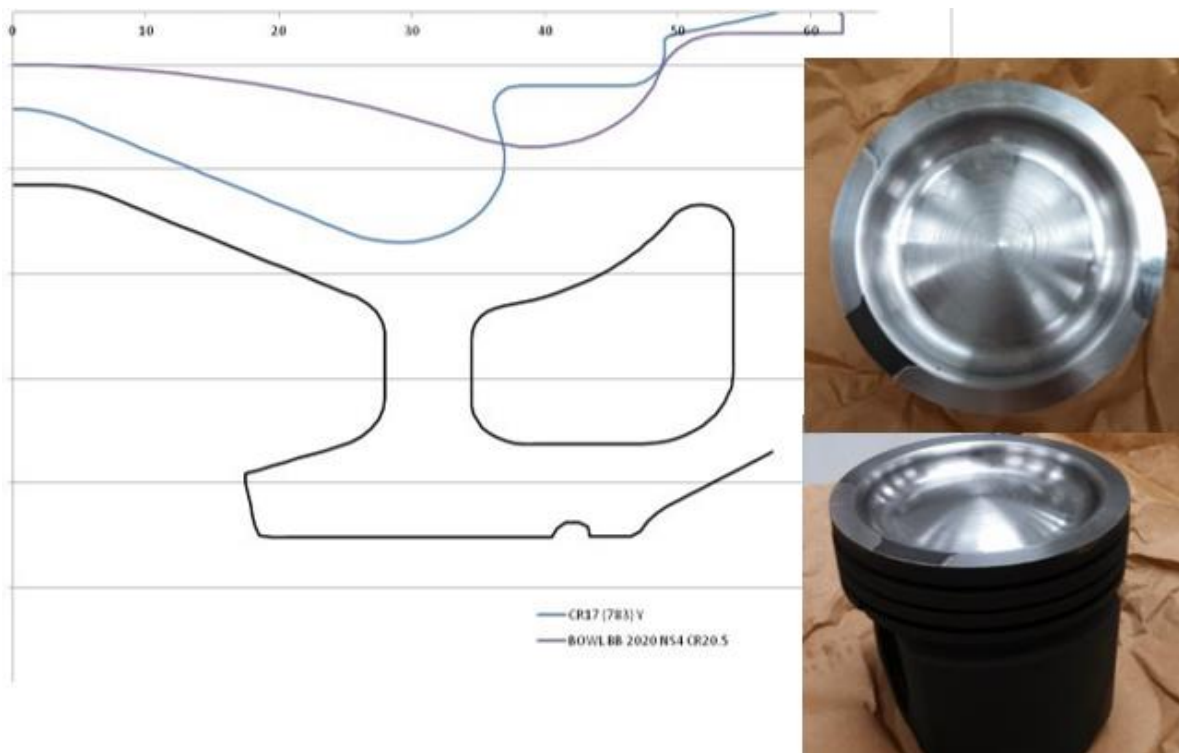
Figure 25: Bowl profile of the 20.5:1 NS4 piston of the Supertruck vs the 2009MY 17:1 piston

With that hypothesis needing to be experimented, bowl-nozzle target testing was performed to find the best the injector nozzle cone angle for spray pattern of fuel to target the piston bowl to maximize its effectiveness. It will be assumed that a wider cone angle will make for better fuel air mixture as well as achieving combustion closer to TDC. For the baseline engine in the 2009MY ProStar, for instance, older "step-bowl" pistons were used as NOx and soot were contained in-cylinder without the need for SCR. Relying on swirl to mix the fuel, air, and copious EGR gases. For the Supertruck, however, engine out NOx was to be increased for fuel economy benefit. Since NOx generation is a product of high temperature and pressure combustion[2] – and the compression ratio and PCP limit of the Supertruck engine is increased,

engine out NOx will increase. After calibration, the tailpipe NOx will be reduced to a legal limit by way of the SCR aftertreatment system.

Cone Angle (°)	Rail Pressure (bar)	SOI (°bTDC)
147	800	14
147	800	12
147	800	10
147	800	8
147	800	6
147	800	14
147	1200	12
147	1200	10
147	1200	8
147	1200	6
147	1200	14
147	1200	12
147	1400	10
147	1400	8
147	1400	6
147	1400	14
147	1400	12
147	1400	10
147	1600	8
147	1600	6
147	1600	14
147	1600	12
147	1600	10
147	1600	8
154	800	6
154	800	14
154	800	12
154	800	10
154	800	8
154	800	6
154	1200	14
154	1200	12
154	1200	10
154	1200	8
154	1200	6
154	1200	14
154	1400	12
154	1400	10
154	1400	8
154	1400	6
154	1400	14
154	1400	12
154	1600	10
154	1600	8
154	1600	6
154	1600	14
154	1600	12
154	1600	10
154	1600	8
154	1600	6

Figure 26: Test Point Matrix for 147 degree vs 154 degree Cone Angle Injector

The first test performed was with 2 cone angles: a 147° cone, like that of the 2009MY baseline, and a 154° cone in effort to maximize the geometry of the wider bowl of the NS4 piston. This test was performed at 300HP, near A75 @ 1040 RPM and 1521 ft-lb of torque. The test swept main injection timing and rail pressure described in the test matrix shown in **Fig 26.** VGT position and EGR valve position remained fixed: VGT at 60% and the EGR valve closed (5% as set by the ECU controls). Each injector set is the same flow rate and the same number of holes. The only difference is the nozzle spray cone angle. Some key responses of significance are NOx, Smoke and BSFC, and PCP.

—×— 147 Cone 800 Bar	—×— 147 Cone 1000 Bar	—×— 147 Cone 1200 Bar	—×— 147 Cone 1400 Bar
—×— 147 Cone 1600 Bar	—×— 147 Cone 1800 Bar	—◆— 154 Cone 800 Bar	—◆— 154 Cone 1000 Bar
—◆— 154 Cone 1200 Bar	—◆— 154 Cone 1400 Bar	—◆— 154 Cone 1600 Bar	—◆— 154 Cone 1800 Bar
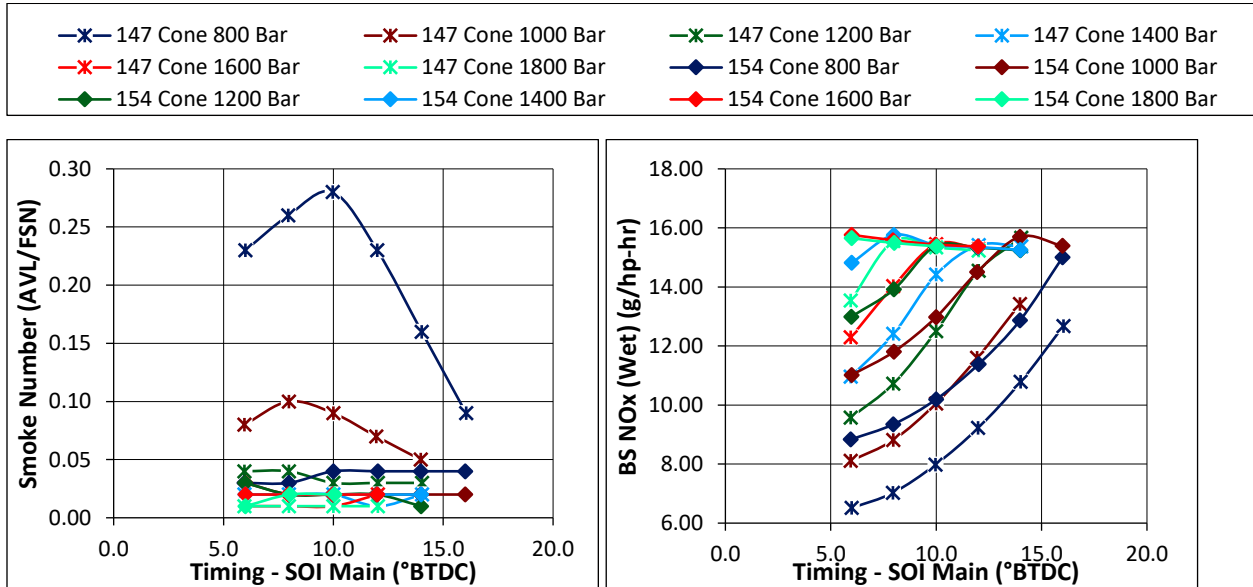
Figures 27a and 27b: Smoke and NOx Response- 147° Cone Angle vs 154° Cone Angle
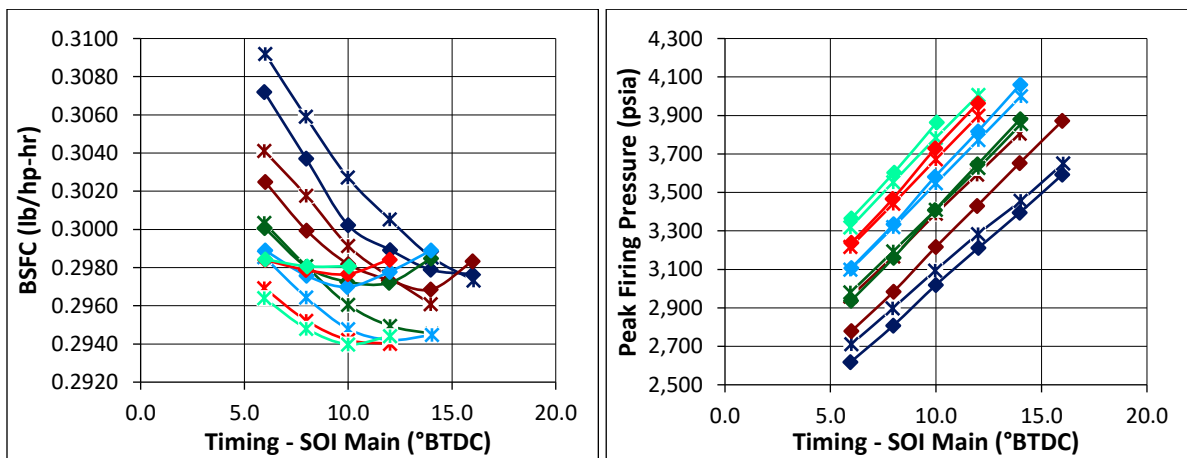
Figures 27c and 27d: BSFC and PCP Response- Narrow vs Mid Cone Angle

Beginning with **Fig. 27a**, smoke number vs the test parameter, SOI. Like the selective catalyst reduction, a diesel particulate filter (DPF) is also a part of the exhaust aftertreatment system. The DPF traps the particulate matter (from smoke) and when exhaust temperatures are high enough, they burned off from the DPF. A smoke number of 1 is the calibration limit, as at that

level, the soot flow becomes high enough that it begins to plug the DPF quicker than it can be burned under normal driving conditions. All the smoke numbers fall well below the value of 1 and show not to be a concern. A low smoke number correlates with NOx levels, which can be examined in the plot shown in **Fig. 27b**. The higher NOx levels correlate with the higher pressure combustion reaction. The BSFC trend in **Fig. 27c** correlates with the ideal response of the Supertruck combustion system, as well. The BSFC decreases as the SOI is advanced, and the rail pressure increases, thereby moving combustion reaction closer to TDC and thus reacting at higher pressures. The measured cylinder pressure trends in **Fig. 27d** begin illustrate the expected response of the new combustion system. Increasing compression ratio, and moving the combustion reaction closer to TDC result in higher peak cylinder pressure. Those higher pressures are correlate to the BSFC minima.

The Indicom software allows for the ability to further analyze the combustion reaction and analyze its correlation to the BSFC response. The results analyzed are defined in terms of mass fraction burned with respect to degrees of crankshaft phasing. Mass fraction burned 10% is a good indicator of the start of combustion. Assessed in degrees, the measured result is referenced to degree of crankshaft angle phasing; with TDC being 0°. Mass fraction burned 10-90% is a good indicator of the crankshaft phasing, in accumulated degrees, for the combustion cycle to be completed. The reference "deg" is the total of degrees for the combustion cycle. For example, a mass fraction burned 10-90% of 23, indicates it took 23° degrees of crankshaft rotation for the bulk of the combustion reaction to take place. As the number of degrees continues to decrease, the faster the combustion reaction happen. A mass fraction burned 10% or (CA10) of -4° degrees and a mass fraction burned 10-90% of 23° degrees can tell the engineer that combustion effectively started at 4 degrees before top dead center and continued the reaction until 19° degees after TDC.
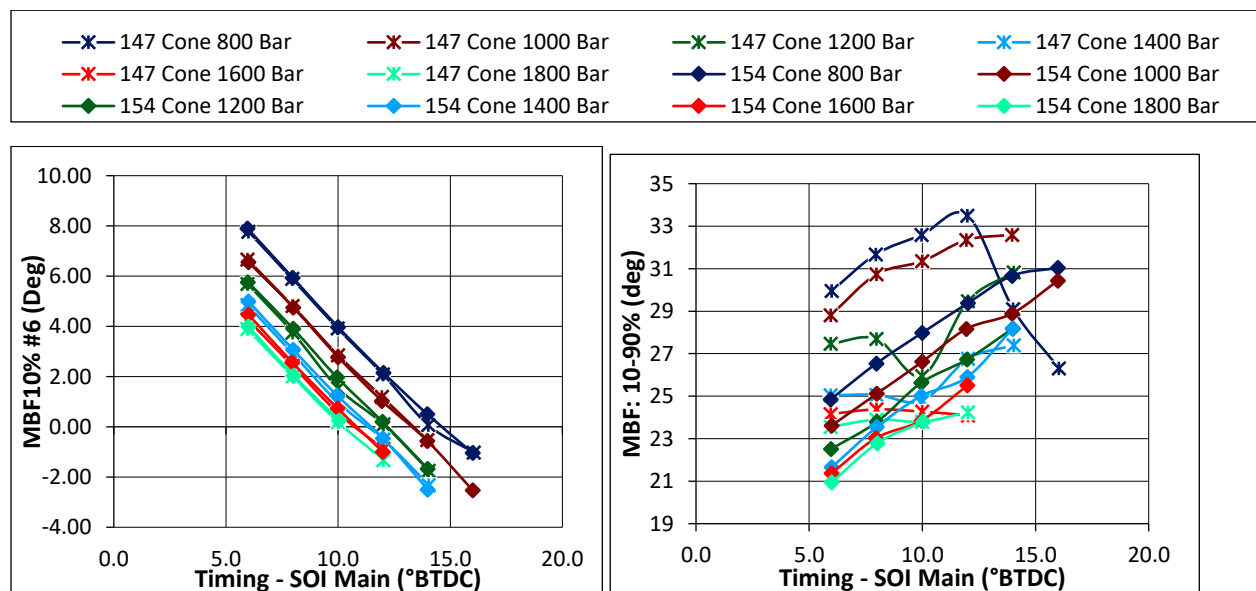
Figures 27e and 27f: CA10 and CA10-90 Response- 147° vs 154° Cone Angle

The graph shown in **Fig. 27e** plots the mass fraction burned of both nozzle sweep configurations. Looking at the CA10 (mass fraction burned - 10%) the start of combustion trends earlier with each step of increased rail pressure. This correlates to the aforementioned peak firing pressure trends and lower trending BSFC. But between the 2 nozzles, there is no difference in CA10 initial combustion. Next, examining **Fig. 27f**, there is a clear trend of decreasing combustion reaction duration, or increasing the rate of heat release, with each increment of increa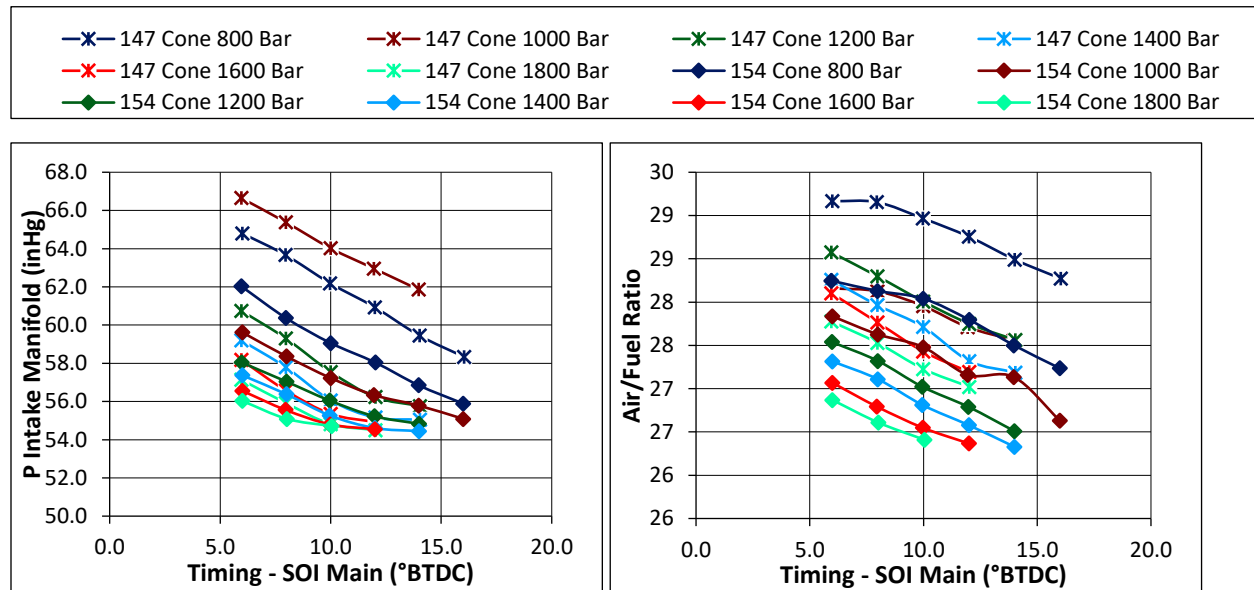sed rail pressure. While there a large difference is shown between the 2 nozzles, in heat release rate, by 1400 bar, the difference has diminished. What the graph does show, is that at 1400 bar and above, there is a convergence at 10 degrees of injection timing. Referring back to **Fig. 27c**, 10 degrees is where there is an inflection point in the BSFC response, as it flattens, and trends upward slightly as the SOI is continued to increase. This shows the combustion reaction is not happening any faster and advancing timing any further begins to go backwards in thermal efficiency benefits to BSFC by reducing cutoff ratio. This information is useful in the calibration effort moving forward.

Although not directly relating to the cone angle comparison, additional knowledge garnered from this test is valuable for the calibration effort. The rail pressure vs NOx vs BSFC relationship will be a delicate balance between peak engine efficiencies, and other constraints of the deliverable; like adhering to the tailpipe NOx requirement. At 15 g/bhp-hr engine-out NOx, the SCR system will need to achieve 99% NOx conversion efficiency to be below a 0.2 g/bhp-hr tailpipe limit. As such, it will be necessary for the calibration to utilize a lower rail pressure, than that which demonstrates the absolute lowest BSFC, to keep the engine-out NOx low enough to work within the constraints of ~97.5% conversion efficiency. Other responses of interest are the impact timing has on turbocharger energy and work done to the airpath system. As timing is advanced, more work is done earlier in the cycle. Although that is the objective of this combustion system, there are negative effects for other components of the system. For example, as the combustion reaction happens sooner in the crank angle phasing domain, exhaust gas temperature is cooler by exhaust valve opening. As a result, work done by the turbine, as a function of allowable exhaust energy available, decreases. The response can be seen in intake manifold pressure (boost) and air fuel ratio; shown in **Fig. 28a and 28b**. The effect on the turbine work and resulting airflow and boost is even more pronounced with the 147° cone injector nozzle. Lower rail pressures mean extended injector ET (energization time) to get the same amount of fuel quantity required to make the same torque as higher rail pressures. Consequently, it is an external impact on actual injection timing, combustion duration, and heat release rate. So, similar effects of retarded timing are seen with the lower rail pressures (along with other responses like smoke or HC). Likewise, referring again to **Fig. 27f**, the slow mass fraction burned 10-90%, of the slowest burn at the lowest rail pressure and 147° cone, is showing a response in energy to the turbo due to the extended combustion duration; or late cycle work that is going out into exhaust energy.   The additional exhaust energy correlates to exhaust manifold pressure, seen in **Fig. 28c**. Likewise, that additional energy available to the turbine is what correlates to the air fuel ratio response, as a function of the increased compressor pressure ratio, seen in **Fig. 28d**.   Because the engine still needs to

promote drivability, as well as adhere to the emissions constraints of the Federal Test Procedure – Emission Cycle (or FTP), when building the engine calibration, will likely be necessary to have an injection timing slightly more retarded than that showing the minimum BSFC to achieve better response from the turbocharger.

—✕— 147 Cone 800 Bar	—✕— 147 Cone 1000 Bar	—✕— 147 Cone 1200 Bar	—✕— 147 Cone 1400 Bar
—✕— 147 Cone 1600 Bar	—✕— 147 Cone 1800 Bar	—◆— 154 Cone 800 Bar	—◆— 154 Cone 1000 Bar
—◆— 154 Cone 1200 Bar	—◆— 154 Cone 1400 Bar	—◆— 154 Cone 1600 Bar	—◆— 154 Cone 1800 Bar

Figures 28a and 28b: Intake Manifold Pressure and Air Fuel Ratio vs SOI - 147° Cone Angle and 154° Cone Angle
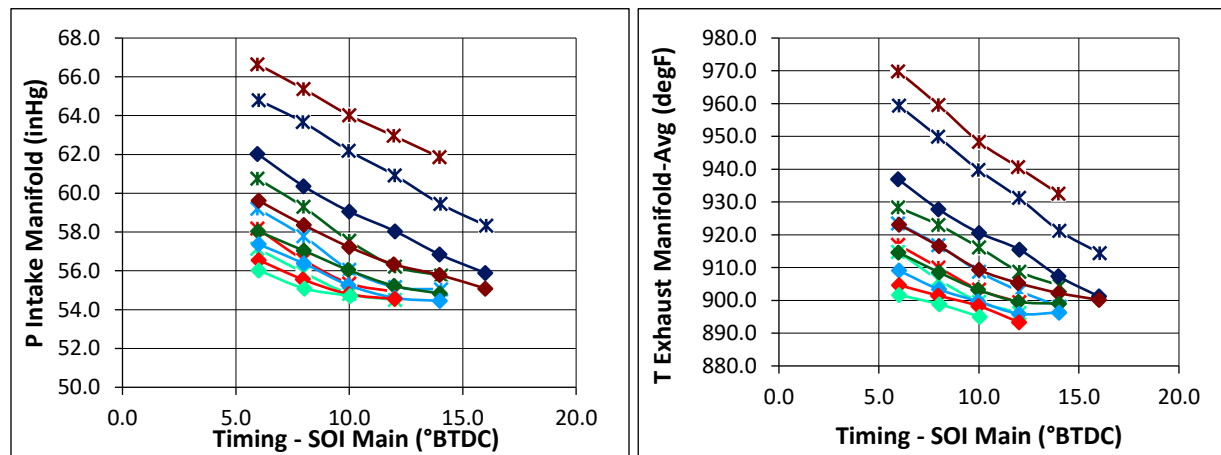
Figures 28c and 28d: Compressor Pressure Ratio and Exhaust Manifold Temperature vs SOI 147° Cone vs 154° Cone Angle

From this test, the response that is found to be counterintuitive to the hypothesis are the results of the injector cone angles themselves. Due to the experimental nature of Supertruck, there are nuances that can affect development process. Once such nuance is product availability and lead time. With the hypothesis of a wider cone angle maximizing the effect of the NS4 piston design, a wider cone angle than what is normally available was also to be tested. However, supplier delays pushed the testing of the nozzle set out, preventing them to be tested

at the same time as the 147°, and 154°. Nevertheless, utilizing the knowledge gained from the earlier test of 147° vs 154° as well as emissions test cycle results from calibration iterations that had ran by this point, a smaller and more concise test was performed with 158° cone angle injectors vs the well-performing 147° cone angle injector set. Since such a crucial point of the freight efficiency improvement goal is the highway cruise point, this comparison was conducted at 200HP closer to the cruise point of A50; at 1054RPM @1003 ft-lb. This test also kept EGR valve position closed but locked VGT position at 55%. This main difference in this test methodology is that it only utilized 1 rail pressure – 1000 bar.   By this point, that was the ideal rail pressure that met the metrics of both fuel consumption and transient performance. This test swept SOI at from 6-16 °bTDC. The results from the test can be seen in **Figs. 29a-f.** There is a clear response from BSFC, of over a 1% reduction with the 158° cone angle injectors, over the 147° cones. Peak cylinder pressure trends higher with the 158° cone, a higher engine out NOx would most likely be expected.
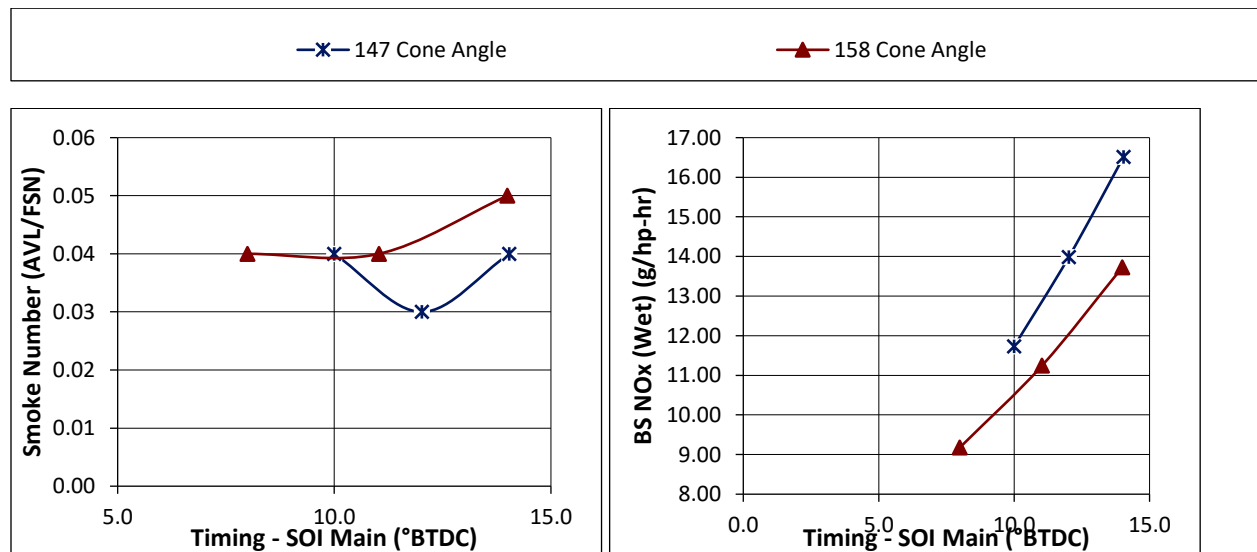
Figure 29a and 29b: Smoke and NOx Response – 147° cone vs 158° Cone
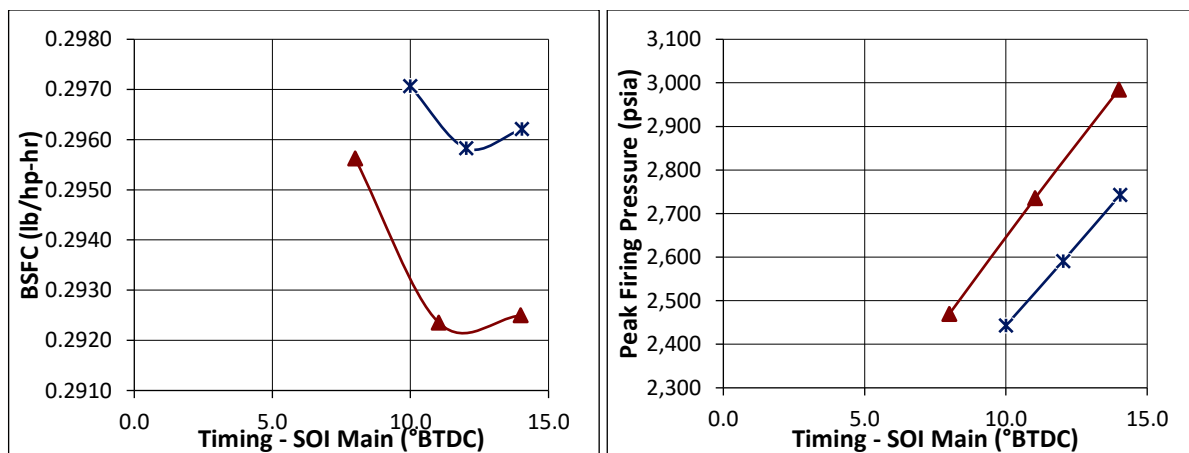
Figure 29c and 29d: BSFC and PCP Response – 147° cone vs 158° Cone

33

The smoke number remains low with the 158°cone. With a better fuel conversion efficiency assumed from the better utilization of the bowl-nozzle match; yielding the improved BSFC; a there is a clear descending trend in the combustion duration from CA10-90 as seen in **Fig. 29f.** from the 158° injector cones.   All of the responses validate the widest cone angle to be a favorable match to maximize the high-flow, low swirl cylinder head and wide shallow bowl of the NS4 piston.
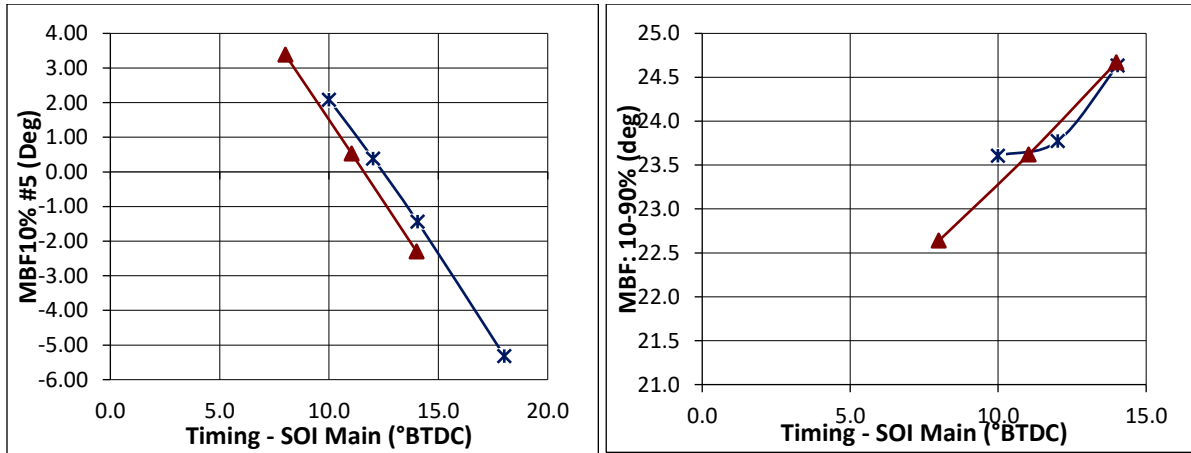
Figure 29e and 29f: CA10 and CA50-90 – 147° cone vs 158° Cone

The NOx trended lower for this comparison which is counterintuitive to a typical response. It should be noted, for the test with the 158° cone angle, there was a small post injection for each point tested on the timing sweep. Throughout this work, numerous tests were done, one of which was a post quantity sweep. This test was done at the same 300HP point as before. With locked rail pressure locked at 1000 bar, the EGR valve set closed, and the VGT position locked position locked at 55%. For this test, post quantity was swept from 0-18 mg/stroke.
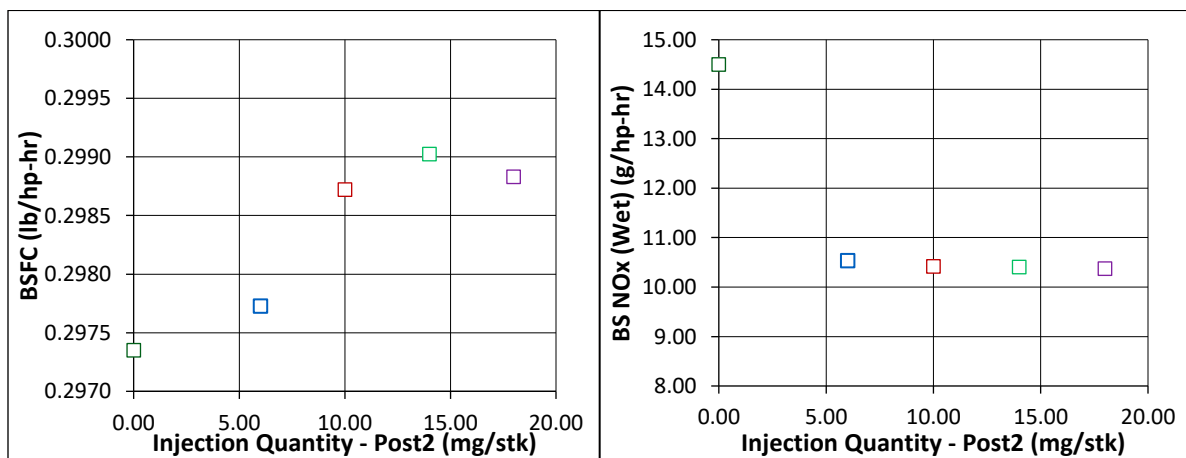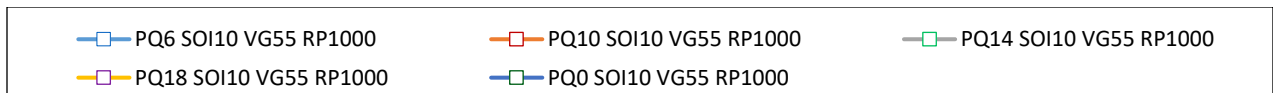
Figure 30a and 30b: BSFC and BSNOx Response – Post Quantity Sweep

It can be noted that there is a very minimal impact on BSFC from any of the post quantities and from 0-6mg/stk there is only a .1% difference in BSFC. And less than a .5% difference total, from the highest and lowest values.   Since the .5% difference shown is actually incrementally positive to BSFC with the addition of 14mg/stk of post injection fuel quantity vs zero quantity on this test, the reduction in BSFC from the 147° cone angle to the 158° cone was the effect of the bowl nozzle target and not the addition of post quantity to the injection scheme. In addition, it can be seen in **Fig. 30b** that the addition of adding a post quantity lowers the NOx substantially with no discernable response to any further NOx reduction after the first 6 mg/stk of fuel is introduced. Hence the reason for the addition of post injection to the injection scheme for the final Supertruck engine calibration, where useful.

Conclusion

While searching for the correct bowl-nozzle match the 154° cone angle did not perform as well as the 147° injector. Showing that the bowl-nozzle targeting is not as simple as wider is better. The fuel injector plume likely hit an unfavorable area on the injector bowl, affecting full utilization of the fuel:air mixture, not promoting the design of the wide and shallow NS4 piston bowl. If a wider cone angle was unavailable, the results would have shown that the 147° cone angle should be used instead, although counter-intuitive to the design of the bowl. However, with the additional test results attained with the 158° injector nozzles that were made available, the hypothesis of a wide injector cone being the best nozzle match for the piston bowl, could be validated.   The lower BSFC and increased HRR from CA10-90% support the conclusion that the proper bowl nozzle target was reached with the widest cone angle.   In addition, the results also validate the combustion schema for the Supertruck engine. Increasing the cylinder head flow and reducing swirl, increasing compression ratio, raising fuel pressure, and widening the injector plumes promote more instantaneous combustion, closer to TDC. The effect of which increases heat release rate, and lowers the cutoff ratio, effectively increasing the brake thermal efficiency of the engine and reduces fuel consumption.

Chapter 3 – Turbocharger Selection

From the waterfall, a third pillar of BTE reduction comes from flow optimization. To compliment the improvements made to the cylinder head, the intake airflow and as a result, the air:fuel ratio, is to be increased. This will be achieved by increasing the airflow output from the turbocharger. However, for that to be effective, the turbocharger must improve efficiency, otherwise the improvements to combustion efficiency will be negated by pumping losses. The modern turbocharger not only increases the work capability of the engine per displacement, but also acts as a knob that can be used to influence NOx and soot responses from the engine. So, within the constraints of engine dP, EGR flow, and engine-out NOx reduction, as the turbocharger's efficiency increases, its ability to drive EGR will also be a factor in the final selection. The 2009MY utilized an R2S turbocharger - or a dual-sequential turbocharging system - utilizing a low-pressure turbo, an inter-stage water to air cooler, and a high-pressure turbocharger. This methodology results in higher engine dP which was necessary to reduce NOx emissions in-cylinder (rather than with SCR). The Supertruck utilizes a variable geometry turbocharger, which allows for the turbo to be sized for peak horsepower, but still maintain favorable low speed, and high-altitude characteristics. The ability to close the vanes, means the flow area of the turbine housing can be slightly smaller than a fixed geometry turbo, so that exhaust energy at low speeds still provides adequate work to react quickly enough to spin the compressor wheel and make boost. This is favorable for engine performance and driver feel. When exhaust flow is high, the vanes can be opened so some of the exhaust energy by passes the wheel and thus doesn't cause a turbo choke or wheel over-speed condition, which is harmful to the turbo and performance.   Therefore, the turbo can give the best of both worlds, at low speeds turbo lag can be reduced, yet peak power isn't reduced due to flow limitations from turbine wheel and housing sizing.

Thus, selecting the proper turbo is critical to overall vehicle performance, fuel economy, and emission responses. Some things to take into consideration are back-to-boost (back-to-boost meaning exhaust manifold pressure to intake manifold pressure) reactions from the size and restriction of the turbo, and efficiency of the turbo, which can alter the turbine outlet temperatures. Positive back-to-boost pressures are necessary because the engine needs to be able to push EGR flow into the intake air stream. If intake manifold pressure is higher than exhaust backpressure, intake manifold air would flow into the EGR system. Turbine out temperature is important for aftertreatment constraints. A turbo is a form of waste heat recovery. If a turbo is very efficient at converting the waste heat across the turbine it is converting much of the exhaust energy into work to spin the compressor wheel. The effects of this are two-fold. Since a diesel engine does not have a throttle, air-fuel ratio, and thus power is only determined by the amount of fuel injected. If a turbo is capable of more boost, and thus higher air flow, exhaust temperatures will be reduced. Additionally, if an efficient turbo is able to convert more of the exhaust energy, turbine out temperatures will be further reduced. The more delta T across a turbine, the more efficient the turbine is. So, all these factors must be considered when selecting the turbo for the Supertruck.

A turbo comparison was performed of 3 experimental turbos, the HET turbo, the BV80 ball bearing, and the I335. The HET turbo, being fixed geometry, and the other 2 being variable geometry.   As stated previously, for Supertruck, the cruise speed (A50) region is most important for real-world fuel economy. As such, this test was performed at a speed and load of 1039 RPM and 1029 ft-lbs of torque. For the test methodology, the vane position of the VGT turbos were locked at 50%.   The fuel rail pressure was locked to 1000 bar. No Post injection fuel quantity was used. The EGR valve position was swept at 5% (fully closed), 25%, 50%, and 95% (fully open). This EGR valve sweeps were then performed at 3 SOI intervals, 10°, 13°, and 16° bTDC. The test point matrix is shown in **Fig. 31**.

SOI (°bTDC)	EGRv (%)	Rail Pressure (bar)	VGT (%)
10	5	1000	50
10	25	1000	50
10	50	1000	50
10	95	1000	50
13	95	1000	50
13	50	1000	50
13	25	1000	50
13	5	1000	50
16	5	1000	50
16	25	1000	50
16	50	1000	50
16	95	1000	50

Figure 31: Test point matrix performed for each turbocharger

Some important responses examined are BSFC, back-to-boost, combined turbo efficiency, and turbine out temperature. However, things like EGR flow and air fuel ratio are important to note. Since the turbocharger is critical to engine-out NOx response, the plots in the following figures are analyzed in the domain of BSNOx; which is the the X-axes. **Fig. 32a** and **32b** show the impact on air:fuel ratio and BSFC. **Fig. 32c** and **32d** show the effect on the exhaust manifold pressures and turbine out temperatures.

Notice the relationships between the responses in the plots above. An initial take-away is independent of the turbochargers; that is the impact of SOI on NOx. As timing is retarded, NOx formation is diminished. This is because peak firing pressure shifts further past TDC. The closer peak firing pressure (peak expansion) is to TDC, the higher the temperature and pressure of the reaction. The higher combustion temperature and pressures yields higher NOx formation. However, also notice that advancing timing decreases BSFC. This also for the same reason; which can be referenced in the equations in chapter 2. It can be observed that the I335 turbo has the lowest AFR and yields the highest BSFC. Correspondingly in **Fig. 32c**, the lower AFRs also give the lowest exhaust manifold pressures, apart from the fixed geometry, HET, turbo.
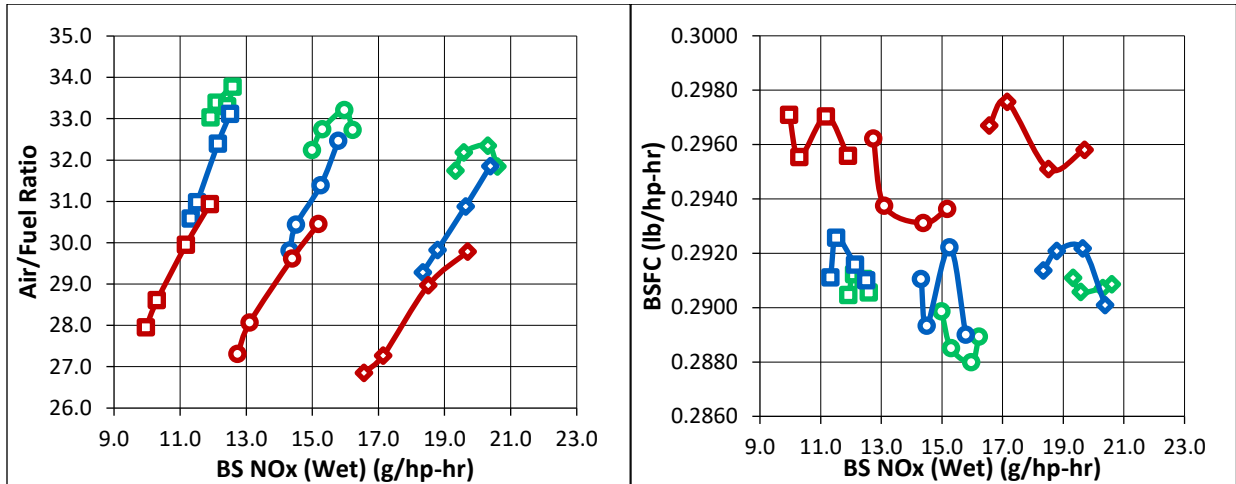
Figure 32a and 32b: Air:fuel Ratio and BSFC vs NOx for the 3 turbos
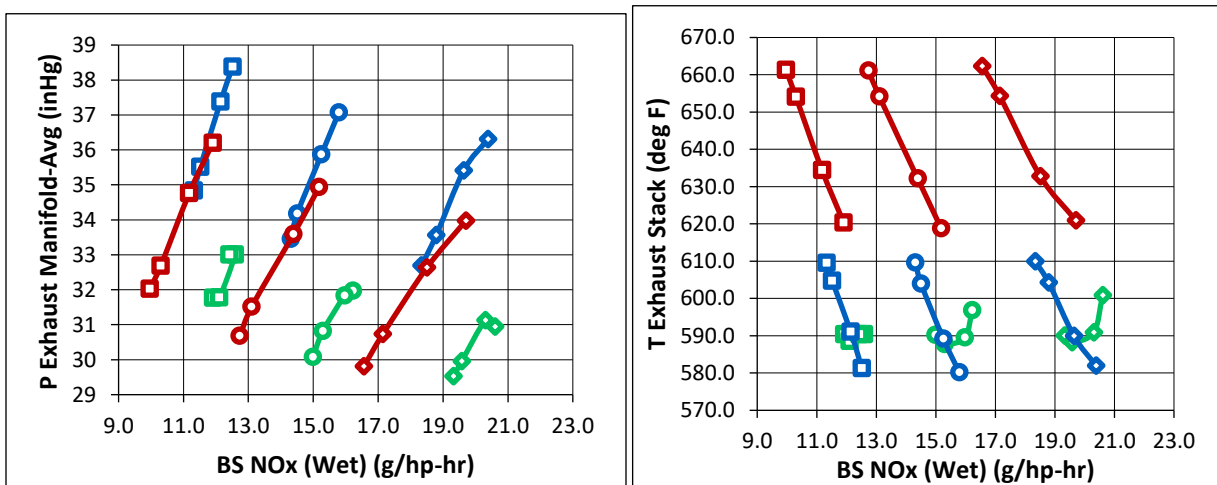
Figure 32c and 32d: Exhaust manifold pressure and turbine out temperature for each of the 3 turbos.

This, combined with the small reactions from the incremental opening of EGR valve position, indicate a difference in the turbine housing size of the HET. Which correlates to the response of the exhaust temperature in Fig. 32d. For the VGT turbos, the lowest AFR prove higher exhaust temperatures, and decrease as EGR valve is opened. But once again, the response is very flat from the HET turbo. The results are further explained with **Fig. 33a and 33b** the responses of EGR flow and back-to-boost can be seen. Even as the EGR valve is opened the back-to-boost is very flat from the HET, and as result, the EGR flow response is both flat, and lower than that of the VGT turbos. If BSFC was the only deliverable, then the comparison would be concluded with the favorable BSFC response from the HET turbo. To the contrary, the back-to-boost and

the resulting EGR flow rate show the downside of this turbo. This turbo was selected as an option due to its efficiencies. However, a consequence of its efficiency is an inability to drive EGR at the lower exhaust flow region of the engine map. Since the Supertruck engine map has shifted to run at lower speeds, which result in lower flows, meeting the 0.2 g/bhp-hr NOx emissions limit on cycle emissions tests could prove difficult with the HET fixed-geometry turbo.

□ phiMI 10, tiPol -950, qPol 0, RP=1000 (HET)	◇ phiMI 13, tiPol -950, qPol 0, RP=1000 (HET)
◆ phiMI 16, tiPol -950, qPol 0, RP=1000 (HET)	□ phiMI 10, tiPol -950, qPol 0, RP=1000, VGT=50 (BV80BB)
◇ phiMI 13, tiPol -950, qPol 0, RP=1000, VGT=50 (BV80BB)	◇ phiMI 16, tiPol -950, qPol 0, RP=1000, VGT=50 (BV80BB)
□ phiMI 10, tiPol -950, qPol 0, RP=1000, VGT=50 (I335VGT)	◇ phiMI 13, tiPol -950, qPol 0, RP=1000, VGT=50 (I335VGT)
◆ phiMI 16, tiPol -950, qPol 0, RP=1000, VGT=50 (I335VGT)	

Figure 33a and 33b: Back-to-boost and resulting EGR flow for each of the 3 turbos

Figure 34: Combined turbo efficiency

The reduction seen to BSFC as well as turbine out temperatures can be linked to the combined turbo efficiency, shown in **Fig. 34**. To maximize the new combustion schema for Supertruck, the airflow is to be increased. But that cannot come at the expense of PMEP. Thus, the turbo efficiency needs to improve as well as increase air flow capability. The ball bearing turbo provides 3% better combined efficiency than the I335. At at this speed 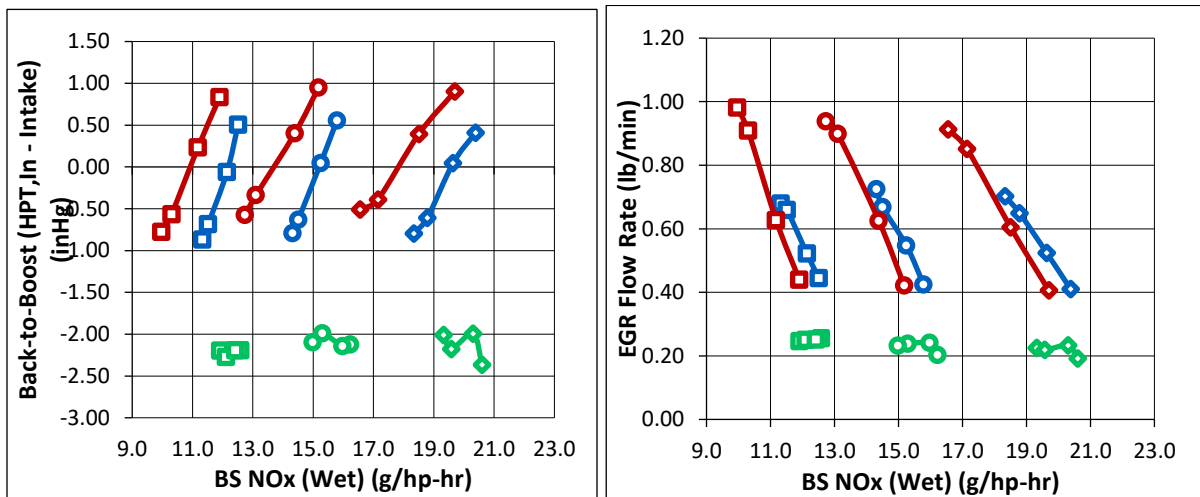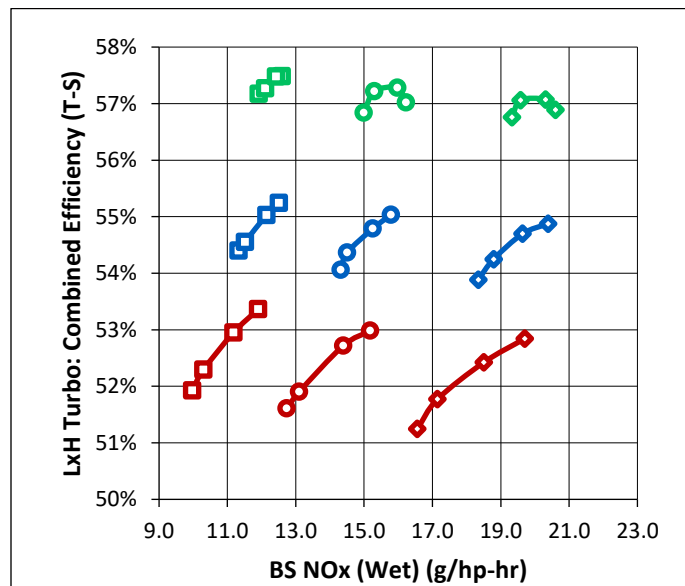and load, the HET is 3% better than the ball bearing. All of these turbos achieve high flows and resulting high air:fuel ratios. But one turbo fits the best within the constraints of Supertruck. The I335 showing the lowest BSFC, makes the HET or BV80BB turbo a better choice. Although the HET turbo shows markedly better combined efficiency, it's inability to respond to changes in EGR valve position at lower engine speeds and loads – where the Supertruck is to run - and effectively reduce NOx, prevent it from being a viable option for Supertruck. Therefore, the ball bearing turbo was selected as the best option for the T4 Supertruck.

When progressing through the development process, it is important to note the responses and incremental changes taking place. When combining the final hardware for the T4 Supertruck, it was fundamental to compare the ball bearing turbo selected for T4, to the turbo utilized for T3. The only difference between the T3 turbo and the ball bearing turbo, was the ball bearing journal, vs the standard oil bushing journal. So, to see the improvement possible from the ball bearing journal, a test was performed sweeping EGRv at 5%, 25%, and 55% with the following additional setpoints in the test matrix shown in **Fig. 35**:

SOI (°bTDC)	EGRv (%)	Rail Pressure (bar)	VGT (%)
8	5	1000	55
8	25	1000	55
8	55	1000	55
11	5	1000	55
11	25	1000	55
11	55	1000	55
14	5	1000	55
14	25	1000	55
14	55	1000	55
11	5	1300	60
11	25	1300	60
11	55	1300	60

Figure 35: Test Point Matrix for T3 vs BV80BB Turbo Comparison

The benefits are still noticeable to BSFC and turbo efficiency, seen in **Fig. 36a** and **36b**. Combined turbo efficiency of the ball bearing turbo on the T4 engine only gains about ~0.5% improvement on combined turbo efficiency compared to the T3 turbo. Nevertheless, it retains efficiency when the EGR valve is opened. Meaning, the ball bearing turbo will maintain it's efficiency even when exhaust energy to the turbine is reduced, as it is diverted through the EGR

valve, just like the T3 turbo. What's more, it is achieving this while still decreasing BSFC. The ball bearing turbo yields an aggregate across all tests of about 1% reduction in BSFC.
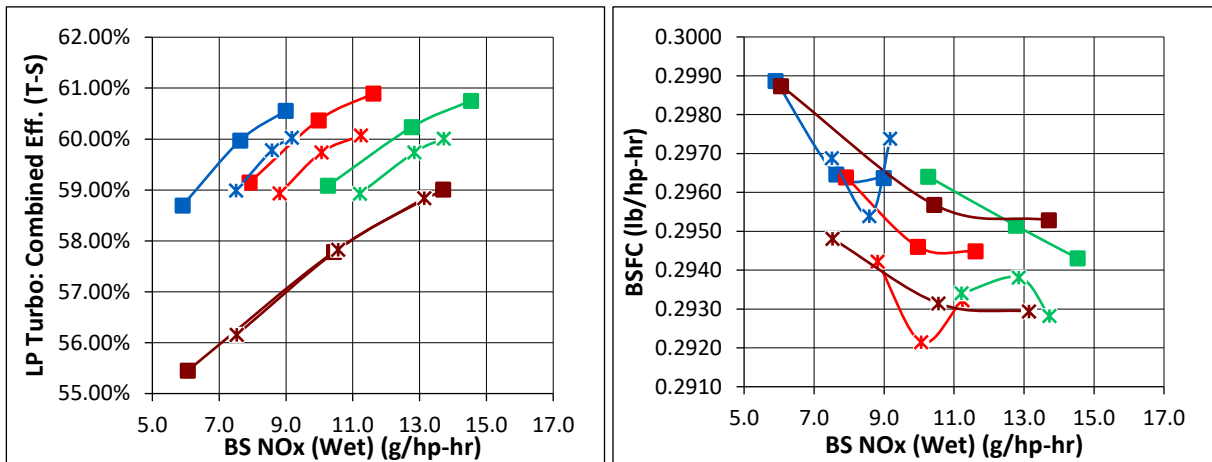
Figure 36a and 36b: T3 turbo vs T4 ball bearing turbo combined turbo efficiency and BSFC difference
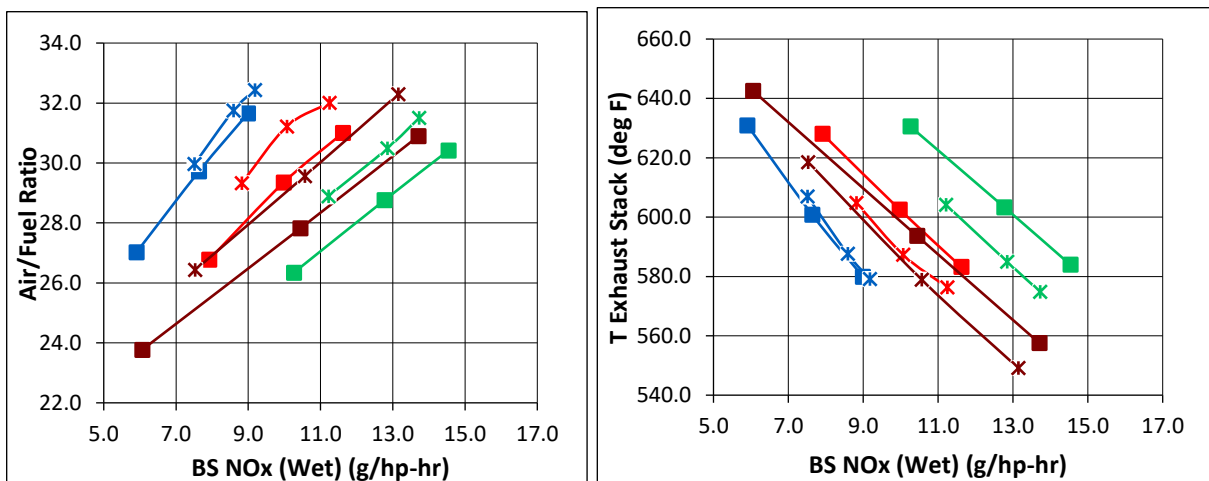
Figure 36c and 36d: T3 turbo vs T4 ball bearing turbo AFR and turbine outlet temperature differences

That 0.5% gain in efficiency is a result of the increased air:fuel ratio yielded from the ball bearing turbo, shown in **Fig. 36c**. As seen in **Fig. 36d**, no appreciable changes to turbine outlet temperature are present due to the increase in air fuel ratio. With temperatures well above a minimum NOx conversion temperature required of roughly 480° degrees Fahrenheit, this small difference will not have any impact to the aftertreatment conversion efficiency.

What's more, the ball bearing turbo still responds to increasing EGR valve in that NOx emission continue to be reduced as the valve opens. The NOx levels are slightly higher than that of the T3 Turbo, as a result of the lower back-to-boost and thus lower EGR flow rate, as shown in **Fig. 37a** and **37b.** But the EGR response is still effective at reducing engine-out NOx.
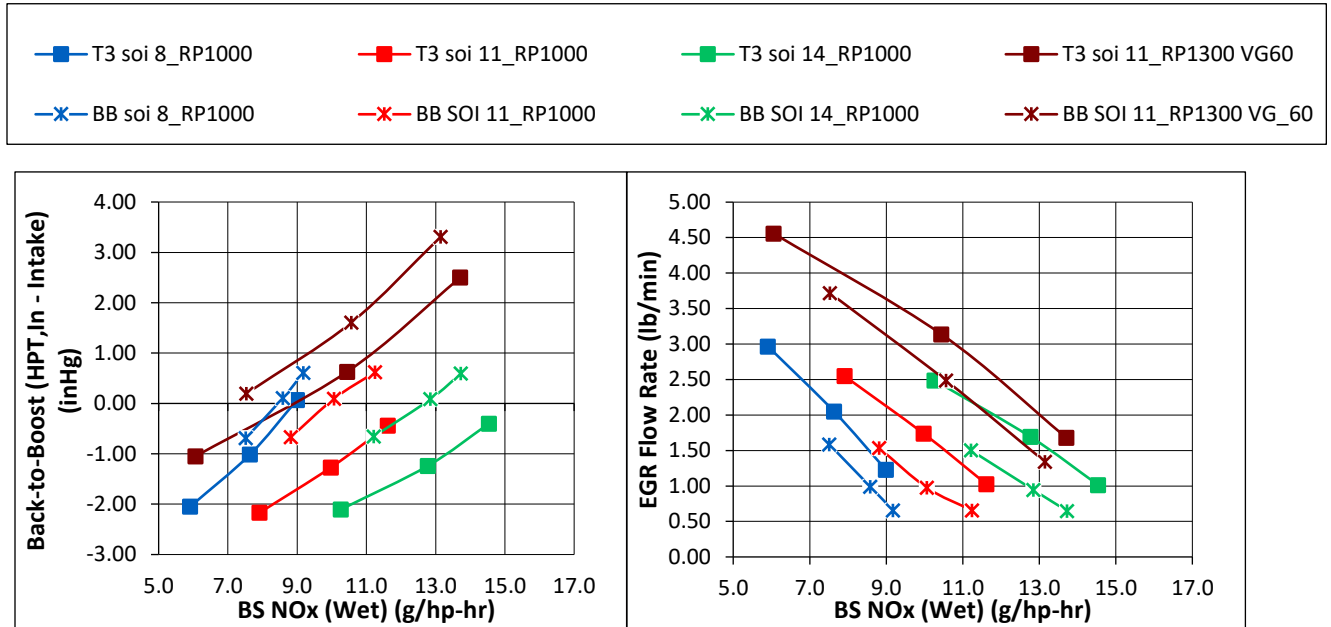
Figure 37a and 37b: T3 turbo vs T4 ball bearing turbo back-to-boost and EGR flow rate

Conclusion:

A considerable amount of work was performed throughout the turbocharger analysis to select a turbo that could be an improvement over the T3 hardware. The HET turbo provided excellent efficiency and BSFC results. But, being fixed geometry, the larger flow area of the turbine showed little response to EGR flow capability at lower engine speeds and loads. With the downsped engine map, the HET will not be favorable to reducing NOx emissions, with the engine-out levels exceeding that which the aftertreatment can reduce. The comparison between the T3 turbo, and the ball bearing turbo showed that the wheels on the T3 were already very effective working in conjunction with the rest of the hardware assembled for the Supertruck engine. Just moving to the ball bearing journal was good for a 1% BSFC improvement with an increase to air:fuel ratio. Ultimately, the turbocharger was a main contributor to pillar of airflow optimization and resulting brake thermal efficiency gain.

Chapter 4 – Variable Water Pump

A variable water pump (VWP) was used on the Supertruck. The variable water pump utilizes an electronically actuated viscous clutch to control the impeller of the water pump at a slower speed than the input speed from the engine belt driven pulley. Since the heat capacity of the cooling system is designed for the peak heat rejection from the engine, slowing the water pump by use of the VWP allows to reduce parasitic losses from the front engine accessory drive (FEAD) at other conditions that do not require as much coolant flow from the water pump. To validate that the VWP can be used to reduce fuel consumption, but still maintain effective cooling a comparison test was performed on a 2009MY production engine. A VWP was installed on the engine and a baseline 13 mode set of data was collected with the VWP at 100% duty cycle, or, at an impeller to pulley speed of 1:1 – like a standard water pump. Then, a 13 mode was performed, manually controlling the duty cycle of the water pump. At A-speed the minimum duty cycle allowed was 40%. At B-speed the minimum duty cycle allowed was 29%. At C-speed the minimum duty cycle allowed was 34%. The limit imposed for this test was a coolant outlet temperature of 230° degrees Fahrenheit. Although a rather basic test, even with unrefined VWP duty cycles selected, there is still a reduction is BSFC. Which is shown in the graph in **Fig. 38a**.
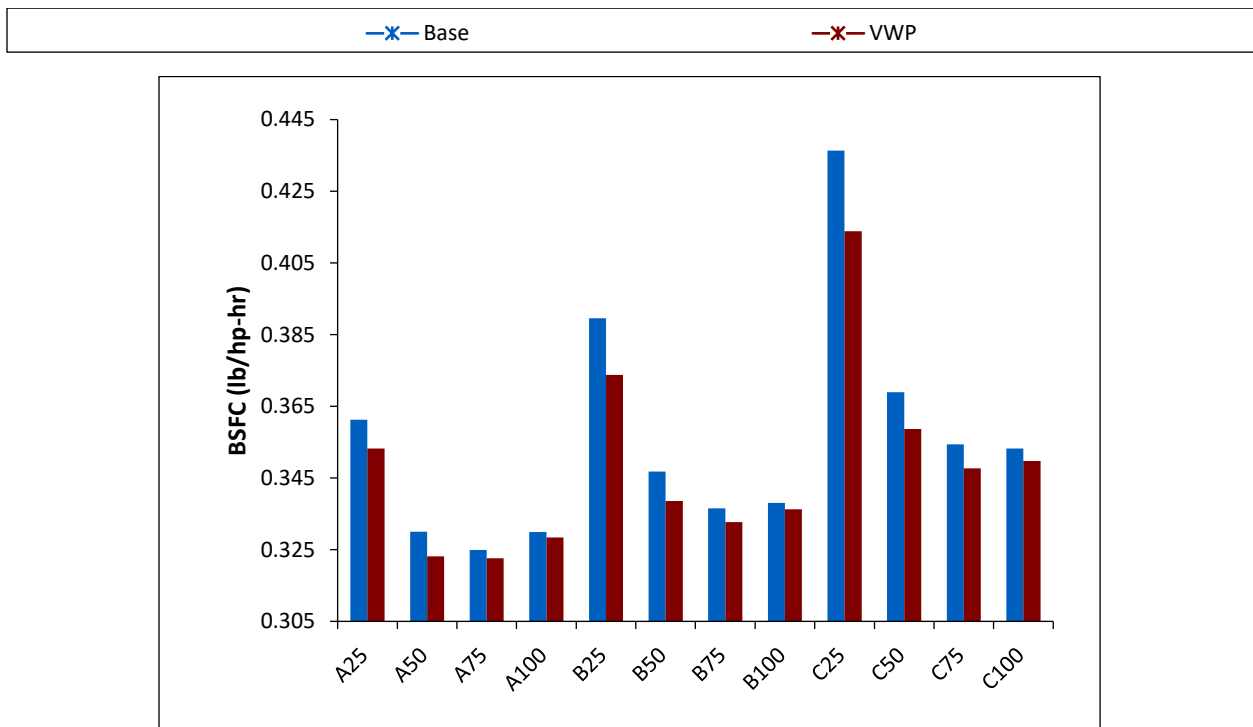
Figure 38a: BSFC comparison of the VWP at 100% duty cycle vs reduced duty cycle
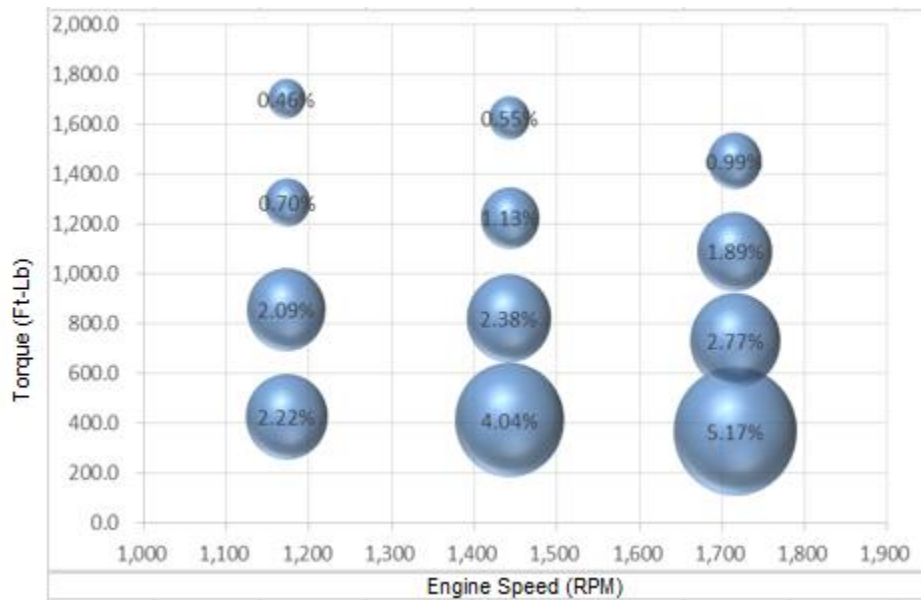
Figure 38b: Percentage of BSFC reduction on the 13 mode points

Notice in **Fig. 38b** at A50, there is the potential for over a 2% BSFC improvement just from slowing down the water pump. This is excellent for highway cruise fuel economy. With this improvement it was important to be sure to study possible unwanted effects as a result of the warmer coolant temperatures. In **Figure 39a** and **39b**, BSNOx and BSSoot responses were compared. The results show an average increase in NOx of 10%, and an average reduction in soot of 2.5%. The range of soot is many orders of magnitude lower than that of concern and thus are inconsequential. With the range of engine-out NOx so low, 10% is also insignificant to the effect on tailpipe NOx.
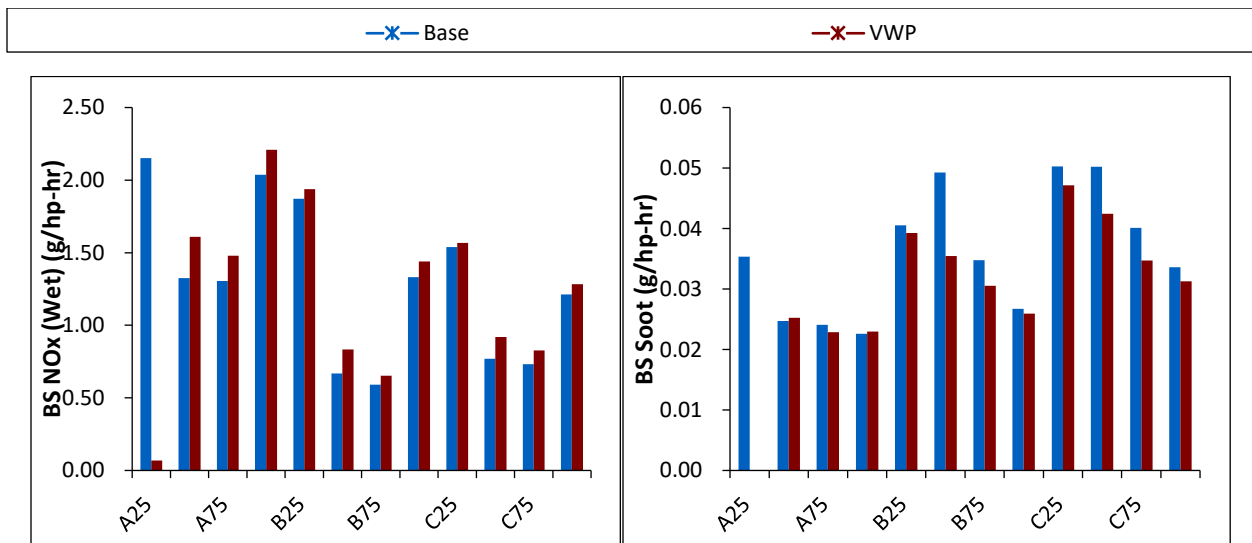
Figure 39a and 39b: BSNOx and BSSoot response from VWP implementation

The EGR cooler gas out temperatures and resulting intake manifold temperatures are important to note and explain the increase to BSNOx. Additionally, oil temperature as well as engine

coolant temperature are also obviously very important to analyze. **Figure 40a** and **40b**. compares the response from EGR cooler gas temperatures and resulting EGRc effectiveness. There does show to be an increase of an average of 19.5° degrees Fahrenheit to gas out temperatures. This is a result of the decrease in EGR cooler effectiveness from the higher EGR cooler gas temperatures. The cooler effectiveness is only reduced by an average of merely 4.5%. There is no hardware limit on gas out temperature, per se. Boiling of the coolant in the cooler must not occur and gas out temperatures must not increase enough such that they raise intake manifold temperature above the limit of 200° degrees Fahrenheit.
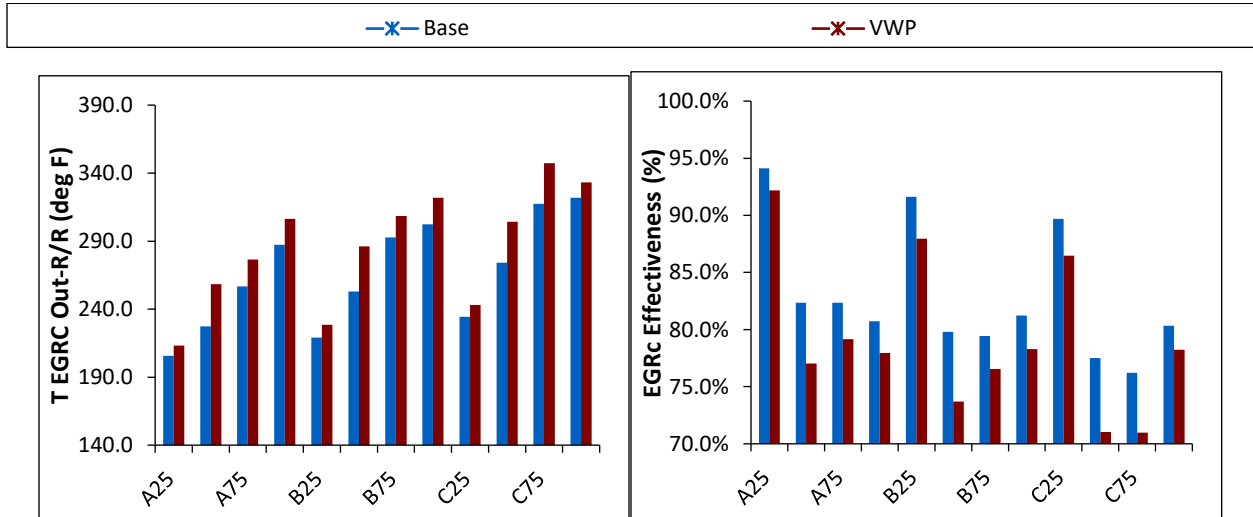
Figure 40a and 40b: EGR cooler gas out and intake manifold temperature response from VWP implementation

The resulting EGR cooler coolant temperature and intake manifold temperatures are shown in **Figure 41a and 41b**. Although a clear increase in EGR cooler coolant temperatures, they remain below the 230F limit.
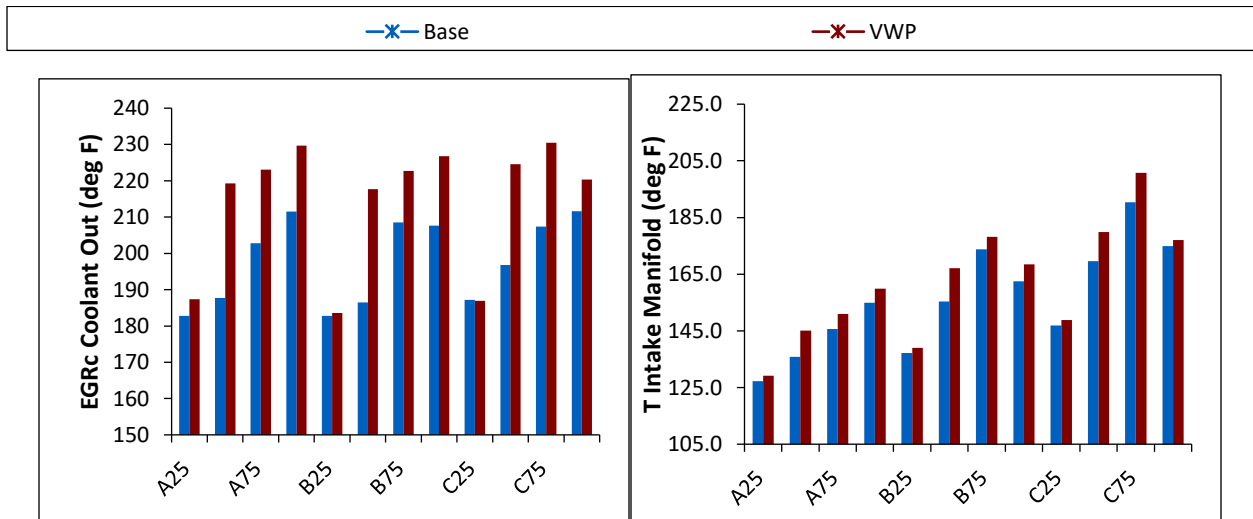
Figure 41a and 41b: EGR cooler coolant out temperature and Intake Manifold Temperature

The result of higher coolant temps, and thus, higher EGR gas out temperatures, does increase the intake manifold temperature; with the C75 point touching the limit at 200° degrees Fahrenheit. But all other points staying below this. **Figure 42a and 42b** illustrate the effect that slowing the waterpump has on coolant and oil temperatures. The coolant shall remain below 230° degrees Fahrenheit and the oil to remain below 260° degrees Fahrenheit. The baseline results show that there is enough heat capacity in the cooling system to leave enough margin to slow the impeller of the water pump and still absorb an adequate amount of heat through the coolant. The results with the VWP do show a clear increase in coolant temperatures, of an average of 16° degrees Fahrenheit, but all points remain below the limit of 230F. Likewise, the oil temperatures are increased by an average of almost 16° degrees Fahrenheit, but all points remain below the limit of 260F.
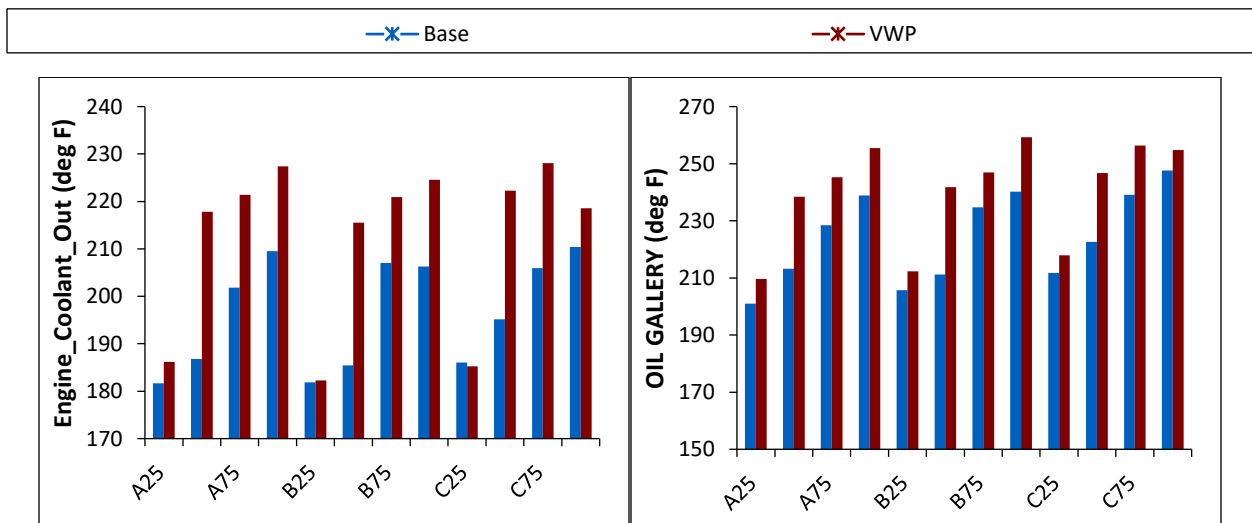
Figures 42a and 42b: Engine coolant out and oil gallery temperatures

230F may seem to indicate localized boiling is possible. But the cooling system of the 2009MY vehicle is designed to run with 15 PSIg of pressure on the system. Moreover, the cooling system of the Supertruck is designed to go even higher by use of an air pressurized system. Using an expansion tank with air pressure from the vehicle's air tanks to hold pressure over the coolant. Setting a pressure of 30 PSIg, this creates even more margin for the VWP. **Fig. 43** shows these same 13M points plotted against the theoretical boiling temperatures, corrected for the factory coolant pressure. With the increased pressure of the coolant system designed for the Supertruck, it will be assured that boiling is not an issue. At 15 PSIg, the boiling point is increased to 264F. At 30 PSIg, the boiling point is raised to 289F. As such, the limiting factor for the temperature response from the VWP will be the oil gallery temperature.
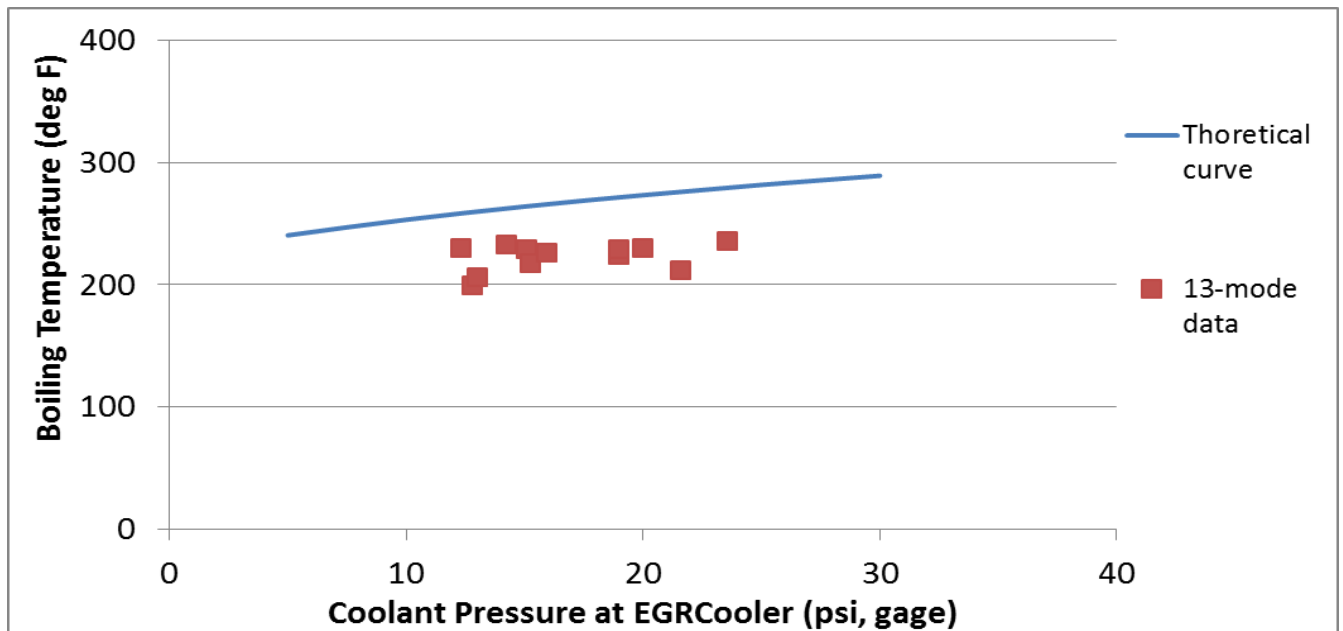
Figure 43: 13M points with slow water pump speed vs theoretical boiling point with the factory coolant degas pressure

Once the Supertruck engine hardware for the T3 truck was assembled the water pump was tested again. This time a 10 point steady state drive cycle sample was used. The drive cycle sample is made by putting a weighting to 10 speed and load points derived from the resonance or dwell time on that particular point of the engine map on the Kentucky Hills and Illinois flat land – per real vehicle driving data. These points are a way to try to quantify real world fuel economy impact with steady state data from the test cell. It is important to note a few things. 1. As mentioned, this was for the T3 truck, so it was not the final vehicle hardware used for the Final Supertruck vehicle demonstration. 2. The data is still in calibration development, and improvement shown is not final (further improvements were made, even with this hardware set) 3. The benefit shown here is versus the 2017 product, that was also still in development stages. This is because the drive cycle sample data wasn't as readily available for a good comparison. Thus, it can be assumed that the difference between the 2009MY baseline vehicle would be even higher. 4. The main take away from **Fig. 44a** and **44b** is to show how much the VWP was able to help decrease fuel consumption on the drive cycle representative of real-world fuel economy – rather than that snapshot of improvement at the time over a development product.

Total of 10 speed/load points capturing 93 % of the long
haul cycle using the 1750 lbf-ft, 450 hp lug curve

1.5 % fuel
economy
improvement
over cycle.
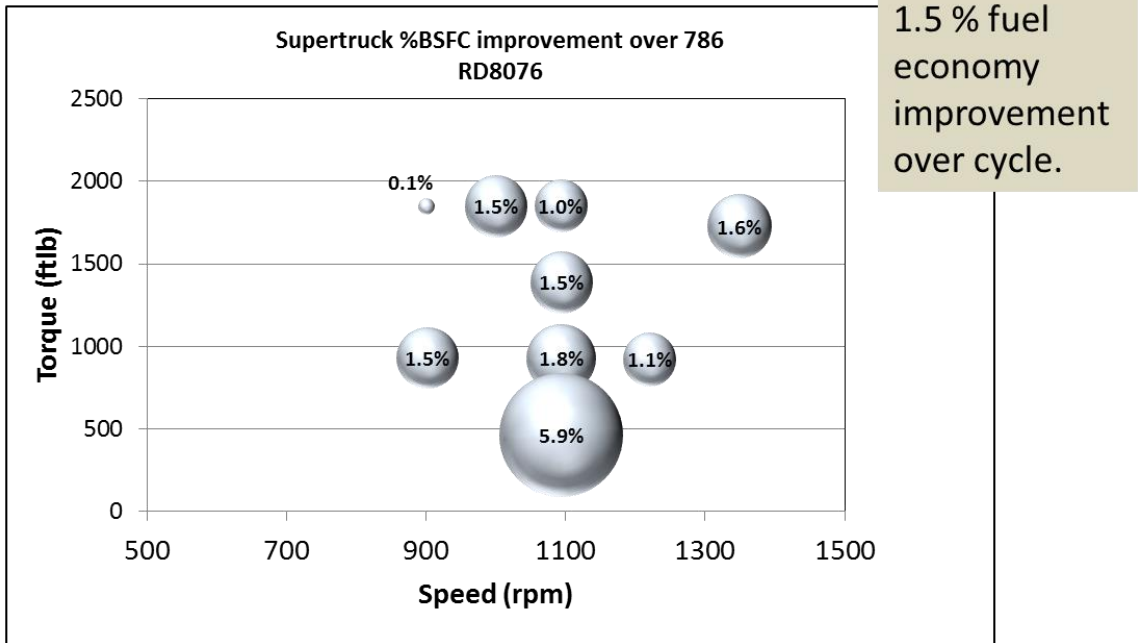
Figure 44a: drive cycle improvement without the water pump: These numbers can almost be seen as a "zero", baseline data, and improvement data are not final numbers.

Total of 10 speed/load points capturing 93 % of the long
haul cycle using the 1750 lbf-ft, 450 hp lug curve

3 % fuel
economy
improvement
over cycle.
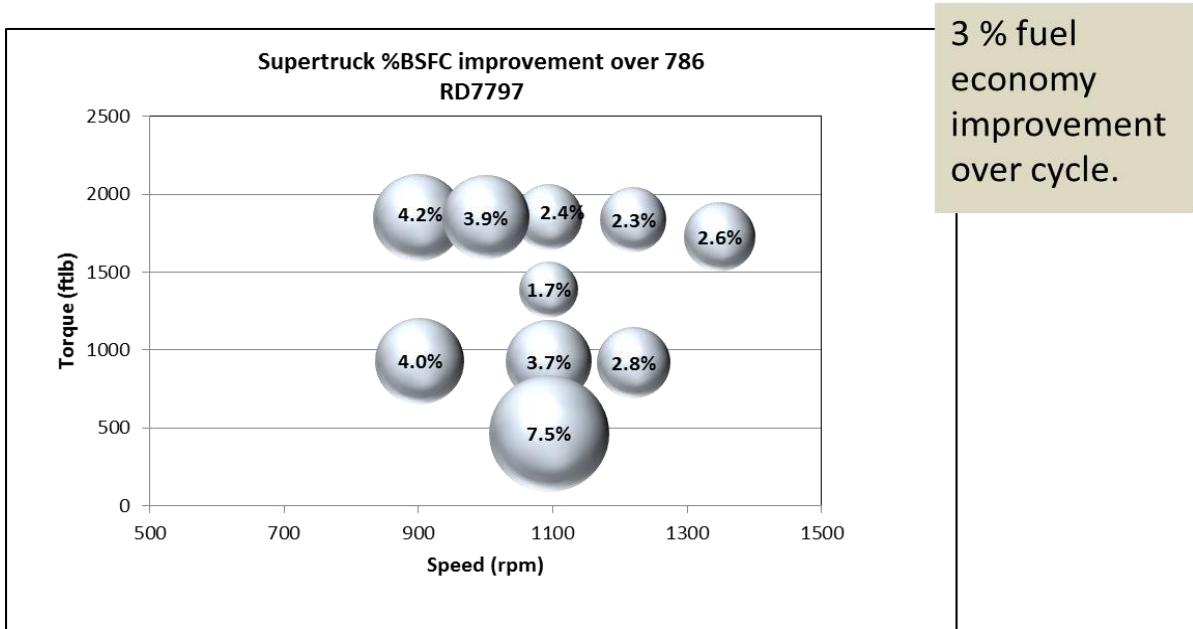
Figure 44b: The water pump gives a 1.5% composite fuel economy improvement over the drive cycle.

Conclusion

Utilizing a variable water pump on the Supertruck was an easy and effective piece of hardware to increase fuel economy. 1.5% fuel economy over the drive cycle is a rather large gain for a single component. The production waterpump flow is designed for worst case scenario heat rejection needs and is oversized for most of the time the vehicle is operating. The use of the VWP still allows for full flow if the demand for cooling is required by the vehicle, for instance, hauling a full load up a mountain in summer. But, hauling a full load down a mostly flat highway, the slower water pump speed can be utilized to increase fuel economy. The water pump was used on the Supertruck, and has since been launched on the production 13L from Navistar Inc.   The data shown in this chapter was from the T3 vehicle development and that engine's progress. The benefit seen was also consistent with the T4 Supertruck final demonstration vehicle.

Final Results and Summary

The results from the T3 demonstration provided a promising progress report on the end goal of Supertruck 1; of 80% freight efficiency improvement.   **Figure. 45** is an image from the Supertruck Final report which shows the T3 progress towards that final goal. This was with a production ProStar tractor seen in Fig. 2, and the modifications mentioned in the Introduction section of this paper.

Figure 45: T3 vehicle progression results
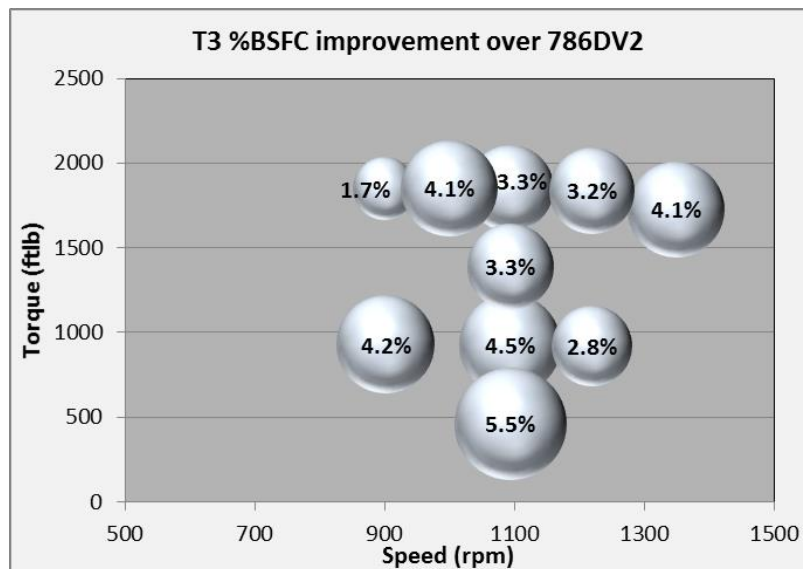
Figure 46: T3 pointwise BSFC improvement over the 2017 development-stage product on the drive cycle sample

The hardware set for the T3 consisted of an early iteration of a high flow, low swirl cylinder head, the 20.5:1 NS4 piston with the 158° cone angle injectors, and a BV80 journal bushing turbocharger. Although the final hardware for T4 still in progress at the time of the T3 demonstration, the calibration developed with this hardware set yielded 4% composite fuel

economy improvement over the 2017 engine, on the 10-point steady state 50/50 drive cycle sample. **Fig 46** depicts the pointwise improvements over the 2017MY development-stage product.

Engine Map Delta Plot T3 vs T4: Turbine Outlet Temperature

CRADLE TORQUE [lb-ft]	700	800	900	1000	1100	1200	1300	1400	1500	1600	1700	1800	1900
1900													
1800				-83.0000									
1700				-93.0000	-84.0000	-72.0000	-67.0000						
1600			-99.0000	-105.0000	-95.0000	-87.0000	-81.0000	-83.0000					
1500			-103.0000	-108.0000	-97.0000	-98.0000	-106.0000	-85.0000	-78.0000				
1400			-97.0000	-107.0000	-99.0000	-110.0000	-125.0000	-92.0000	-81.0000				
1300		-56.0000	-77.0000	-107.0000	-116.0000	-125.0000	-132.0000	-112.0000	-92.0000	-42.0000			
1200		-41.0000	-60.0000	-119.0000	-141.0000	-139.0000	-133.0000	-118.0000	-95.0000	-48.0000			
1100		-37.0000	-49.0000	-134.0000	-148.0000	-141.0000	-117.0000	-114.0000	-105.0000	-51.0000			
1000	-48.0000	-43.0000	-52.0000	-129.0000	-146.0000	-124.0000	-99.0000	-101.0000	-100.0000	-50.0000			
900	-55.0000	-55.0000	-64.0000	-122.0000	-132.0000	-111.0000	-97.0000	-97.0000	-100.0000	-61.0000	-28.0000		
800	-51.0000	-56.0000	-73.0000	-108.0000	-117.0000	-97.0000	-93.0000	-100.0000	-90.0000	-64.0000	-35.0000	-23.0000	
700	-34.0000	-54.0000	-74.0000	-109.0000	-102.0000	-84.0000	-80.0000	-90.0000	-89.0000	-56.0000	-35.0000	-18.0000	
600	-17.0000	-37.0000	-74.0000	-114.0000	-104.0000	-81.0000	-68.0000	-71.0000	-68.0000	-51.0000	-31.0000	-13.0000	
500	-8.0000	-19.0000	-48.0000	-100.0000	-98.0000	-77.0000	-67.0000	-66.0000	-64.0000	-45.0000	-23.0000	-8.0000	-3.0000
400	29.0000	14.0000	-7.0000	-56.0000	-65.0000	-56.0000	-58.0000	-58.0000	-68.0000	-48.0000	-28.0000	-19.0000	-4.0000
300	127.0000	76.0000	43.0000	-15.0000	-31.0000	-17.0000	-27.0000	-65.0000	-77.0000	-59.0000	-41.0000	-41.0000	-17.0000
200	179.0000	102.0000	64.0000	-15.0000	-33.0000	12.0000	2.0000	-68.0000	-71.0000	-62.0000	-47.0000	-46.0000	-31.0000
100	181.0000	113.0000	64.0000	-12.0000	-31.0000	25.0000	11.0000	-56.0000	-70.0000	-63.0000	-51.0000	-44.0000	-36.0000
50	0.0000	0.0000	0.0000	0.0000	0.0000	0.0000	0.0000	0.0000	0.0000	0.0000	0.0000	0.0000	0.0000

Engine Map Delta Plot T3 vs T4: AFR

CRADLE TORQUE [lb-ft]	700	800	900	1000	1100	1200	1300	1400	1500	1600	1700	1800	1900
1900													
1800				2.2000									
1700				1.8000	2.4000	2.8000	2.8000						
1600			2.4000	1.7000	2.0000	2.7000	2.8000	2.6000					
1500			2.6000	1.5000	1.9000	2.7000	2.9000	2.5000	2.5000				
1400			2.4000	1.6000	2.1000	2.9000	3.1000	2.7000	2.4000				
1300		2.5000	2.4000	2.5000	3.2000	3.4000	3.3000	2.7000	2.0000	0.7000			
1200		2.4000	2.6000	4.0000	4.8000	4.6000	3.5000	2.6000	1.8000	0.6000			
1100		2.3000	2.5000	4.9000	5.4000	5.1000	3.9000	2.7000	2.1000	0.7000			
1000	2.7000	2.7000	2.4000	4.7000	5.3000	4.6000	3.5000	2.9000	2.7000	1.0000			
900	3.1000	3.0000	3.1000	4.7000	4.8000	4.1000	3.5000	2.9000	3.9000	2.5000	1.1000		
800	3.9000	3.5000	4.4000	5.7000	5.6000	4.4000	3.7000	2.9000	4.1000	3.3000	1.9000	1.2000	
700	4.5000	5.1000	6.2000	7.0000	6.3000	6.0000	5.4000	4.3000	4.6000	3.4000	2.2000	1.2000	
600	4.6000	5.9000	7.1000	7.2000	6.3000	6.4000	7.1000	6.4000	5.4000	3.7000	2.2000	1.0000	
500	3.3000	4.7000	5.7000	8.0000	7.3000	8.0000	10.3000	9.2000	7.3000	4.5000	2.4000	1.2000	0.6000
400	4.4000	3.6000	6.5000	13.6000	14.2000	15.8000	16.7000	8.6000	8.2000	5.8000	3.9000	3.7000	1.7000
300	6.5000	7.5000	14.3000	23.3000	22.0000	23.3000	26.5000	10.2000	8.6000	7.3000	6.6000	9.2000	4.7000
200	8.9000	15.5000	19.4000	30.3000	24.2000	24.2000	27.2000	12.1000	7.1000	8.2000	8.2000	10.2000	8.1000
100	9.0000	14.7000	19.8000	29.9000	25.8000	23.7000	28.1000	13.4000	7.2000	8.3000	8.8000	9.5000	8.9000
50	0.0000	0.0000	0.0000	0.0000	0.0000	0.0000	0.0000	0.0000	0.0000	0.0000	0.0000	0.0000	0.0000

Figure 47a and 47b: T3 and T4 Engine map deltas: turbine outlet temperature and AFR

Between the August 2015 demonstration with the T3 vehicle, and the following August of 2016 the final turbo analysis and selection was made for the BV80W ball bearing turbo. In addition, the final iteration of the cylinder head, which was projected for the 2017-intent engine, became available and was included for the T4 engine. In addition, the variable water pump, w was also installed on the engine. A complete re-calibration was performed with the final hardware set in

place. The final calibration allowed for even more BSFC improvement. That, combined with the improvements to the T4 vehicle package, allowed for final iteration of Supertruck 1 improvement results. Notice the delta plots of turbine outlet temperature and AFR from the engine maps from the T3 engine and the T4 engine. **Figure 47a** shows the reduction in turbine outlet temperature and **Figure 47b** shows the increase in AFR, both due to the increased efficiencies of the ball bearing turbo; outlined in chapter 3.

Since turbine out temperatures were reduced, there could be an impact on SCR performance. This, due to minimum SCR brick temperatures required for adequate conversion efficiency. Also due to the increase in AFR, and a reduction in the back-to-boost with a more efficient turbo, there is an increase to engine-out BSNOx. **Figure 47a and 47b** show the engine map delta plots for back-to-boost and BSNOx. Notice there is higher NOx almost everywhere, and almost lower back-to-boost almost everywhere. While the increased NOx and decreased SCR inlet temperatures are a detriment to SCR performance, the increased air flow this turbo produces also increases exhaust flow. The increased flow helps SCR conversion efficiency by allowing more ability to suspend DEF in the exhaust stream. The increase in DEF still allows to reduce tailpipe NOx.

Engine Map Delta Plot T3 vs T4: Back-to-Boost

CRADLE TORQUE [lb-ft]	700	800	900	1000	1100	1200	1300	1400	1500	1600	1700	1800	1900
1900													
1800				-1.8000									
1700				-0.8000	-1.3000	-1.8000	-2.1000						
1600			-0.4000	-0.4000	-1.3000	-1.7000	-2.1000	-2.6000					
1500			0.5000	-0.1000	-1.6000	-1.3000	-0.7000	-2.6000	-2.1000				
1400			-0.8000	-0.2000	-1.4000	-0.5000	0.9000	-1.9000	-1.9000				
1300		-4.5000	-2.3000	-0.5000	-0.6000	0.6000	1.3000	-0.5000	-0.5000	1.2000			
1200		-4.1000	-3.3000	-0.3000	0.6000	0.7000	1.0000	-0.5000	0.1000	1.2000			
1100		-4.0000	-3.6000	0.5000	0.9000	0.4000	-0.4000	-1.0000	-0.1000	1.1000			
1000	-2.6000	-3.6000	-3.2000	0.4000	1.0000	-0.2000	-1.4000	-2.4000	-1.1000	0.8000			
900	-1.8000	-1.7000	-2.0000	0.1000	0.5000	-0.7000	-1.6000	-2.9000	-2.2000	-0.6000	0.0000		
800	-1.1000	-0.9000	-0.9000	-0.5000	-0.3000	-0.9000	-1.7000	-2.6000	-2.4000	-1.7000	-0.9000	-0.5000	
700	-0.7900	-0.5800	-0.7500	-0.8300	-0.9000	-1.1000	-1.3000	-2.2000	-2.2000	-2.1000	-1.3000	-0.9000	
600	-0.8200	-0.9800	-0.9000	-1.0200	-1.0000	-0.9000	-1.0000	-1.6000	-2.2000	-2.4000	-1.9000	-1.8000	
500	-0.9700	-1.0500	-1.0200	-0.9300	-0.9800	-0.9000	-0.8600	-1.1700	-2.0000	-2.3000	-2.3000	-2.6000	-2.6000
400	-0.9700	-1.1700	-0.9700	-0.5600	-0.3700	-0.3400	-0.6500	-0.9900	-1.8100	-2.1000	-2.2000	-2.4000	-2.9000
300	-0.6700	-0.8600	-0.6100	-0.0700	0.1560	0.1600	-0.2400	-0.7600	-1.6200	-2.2000	-1.7000	-1.9000	-2.7000
200	-0.4220	-0.5490	-0.4400	0.2030	0.2560	0.3610	-0.0600	-0.7800	-1.3900	-2.3000	-1.5000	-1.6000	-2.4000
100	-0.4070	-0.5240	-0.4400	0.1940	0.2280	0.4350	0.0100	-0.7400	-1.4000	-2.2500	-1.4000	-1.6000	-2.1000
50	0.0000	0.0000	0.0000	0.0000	0.0000	0.0000	0.0000	0.0000	0.0000	0.0000	0.0000	0.0000	0.0000

Engine Map Delta Plot T3 vs T4: BSNOx

CRADLE TORQUE [lb-ft]	700	800	900	1000	1100	1200	1300	1400	1500	1600	1700	1800	1900
1900													
1800				3.4800									
1700				2.0800	2.9300	2.9700	2.8100						
1600			1.0000	1.5000	2.6800	3.0600	2.4400	2.1300					
1500			0.7000	1.3000	2.7400	2.9800	2.0700	2.0700	1.8400				
1400			1.1000	1.4000	2.6200	2.5400	1.5500	1.8700	1.6200				
1300		2.2000	1.6000	1.6000	2.5400	2.0800	1.4300	1.2500	0.6400	-0.2400			
1200		2.2000	1.8000	1.9500	2.5300	2.2800	1.2300	0.5400	0.1000	-0.3200			
1100		2.0000	1.6000	1.8800	2.5600	2.4000	0.8100	-0.0200	-0.0100	-0.2600			
1000	3.8000	2.0000	1.3000	1.8000	2.2400	1.5100	-0.1700	-0.2100	0.2300	-0.0800			
900	2.8200	2.0500	1.7300	1.7800	2.1400	0.7200	-0.1800	-0.2200	0.7500	0.5900	0.1600		
800	2.3400	2.0500	2.2400	2.2100	1.7200	0.4300	-0.0200	0.0100	1.1800	1.0600	0.4800	0.3100	
700	2.1300	2.5000	2.7900	2.6800	1.8700	1.2400	0.7800	0.6800	1.3900	1.0100	0.6000	0.3100	
600	2.1400	2.5600	3.0000	2.8200	1.8800	1.4600	1.4400	1.3200	1.2600	0.9500	0.5300	0.1900	
500	1.9400	1.2700	2.5900	2.8400	2.1400	1.6400	1.9700	1.7000	1.2700	0.7700	0.2600	0.0400	0.0200
400	1.6100	1.0400	2.1800	3.5200	3.5600	3.2700	3.0200	1.9000	1.1700	0.7200	0.3500	0.3100	0.0800
300	2.4300	1.9400	2.9300	4.6100	4.9700	5.1000	4.9100	2.1300	0.8800	0.7400	0.7000	1.0400	0.4400
200	3.2400	2.8900	3.3000	5.3300	5.2300	5.5900	5.5100	2.3300	0.7100	0.7500	0.9000	1.1600	0.9200
100	3.2800	2.9700	3.3500	5.2700	5.3200	5.6700	5.7200	2.5600	0.8200	0.7800	0.9600	1.0700	1.0000
50	0.0000	0.0000	0.0000	0.0000	0.0000	0.0000	0.0000	0.0000	0.0000	0.0000	0.0000	0.0000	0.0000

Figure 47a and 47b: T3 and T4 Engine map deltas: back-to-boost and BSNOx

One thing discovered when going through the calibration effort, was that the increased AFR allowed the ability to add a post injection and get BSFC benefit from late cycle work. The T3 truck engine did not utilize a post injection. **Figure 48** is the contour plot for the post quantity for the T4 engine.
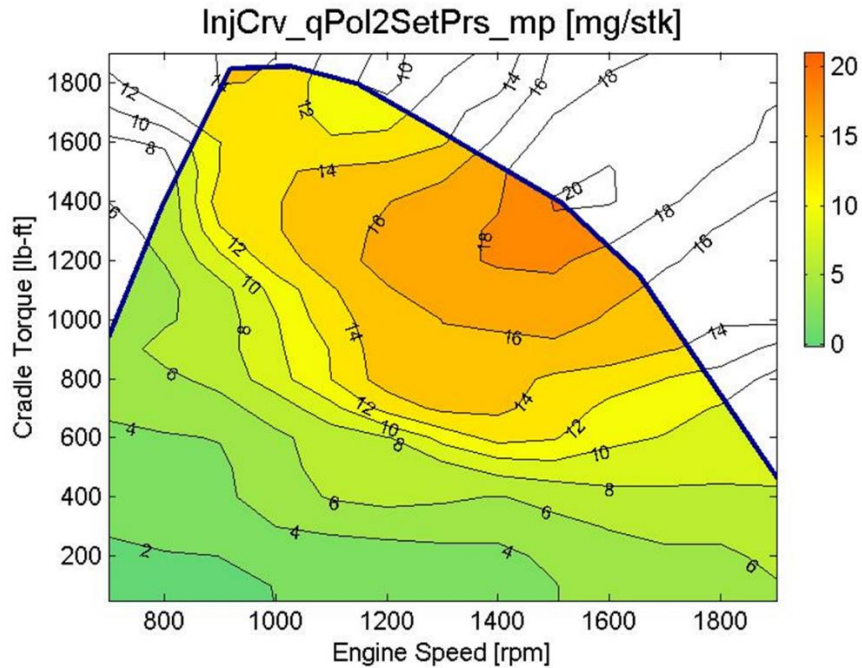

Figure 48: Post quantity contour plot

All of these hardware and calibration changes yielded even further BSFC improvements over the T3 Engine, shown in the engine map delta plot in **Figure 49**.

Engine Map Delta Plot T3 vs T4: BSFC

CRADLE TORQUE [lb-ft]	700	800	900	1000	1100	1200	1300	1400	1500	1600	1700	1800	1900	2000
1900														
1800				-0.34										
1700				-1.01	-1.68	-2.33								
1600			-2.98	-1.69	-1.69	-2.01								
1500			-2.66	-1.02	-1.36	-2.03	-2.66	-3.28						
1400			-2.65	-1.36	-1.36	-2.03	-2.34	-3.29						
1300		-3.23	-2.63	-1.68	-1.69	-2.02	-2.34	-2.65	-1.33					
1200		-2.89	-2.61	-1.67	-1.68	-2.01	-2.01	-1.99	-1.00					
1100		-2.90	-2.29	-1.67	-1.68	-2.01	-1.99	-1.97	-0.99	-0.33				
1000	-2.54	-2.59	-1.97	-1.67	-1.35	-1.99	-1.97	-1.94	-1.31	0.00				
900	-2.86	-2.88	-2.59	-1.99	-2.33	-1.98	-1.96	-2.25	-1.61	-0.65				
800	-2.21	-3.16	-2.55	-2.23	-1.29	-1.29	-1.94	-2.24	-2.23	-0.32	1.26			
700	-0.31	-1.57	-1.88	-2.47	-1.25	0.32	0.00	-1.59	-1.58	0.00	0.93			
600	0.31	-0.31	-0.93	-3.05	-1.24	0.63	2.22	0.30	0.00	0.61	1.51			
500	0.00	0.61	-1.82	-2.08	-0.30	2.82	5.86	5.44	3.12	1.99	2.85	3.14	3.16	
50	0.00	0.00	0.00	0.00	0.00	0.00	0.00	0.00	0.00	0.00	0.00	0.00		

Figure 49: T3 and T4 Engine map deltas: BSFC

Figure 50 depicts the improvement in BSFC over the 10-point 50/50 steady state drive cycle sample. Note, that the T4 engine did not have the VWP on the FEAD, it was just a standard water pump. Even without the VWP, the T4 engine improves BSFC by 1.66% as a composite number over the drive cycle. Adding in the water pump gives at least another 1% for a total of 2.66%. And adding 1% to each of the points in **Figure 50**.
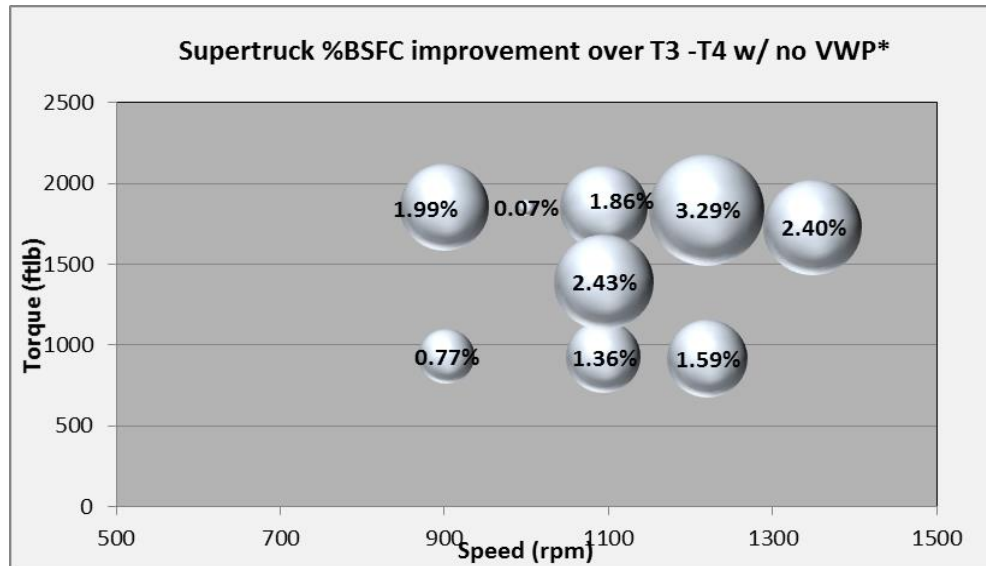

Figure 50: T4 engine improvement on the 10-point drive cycle sample over T3

Figure 51 shows the T4 improvement over the 2017MY development engine. Once again, another 1% can be added to each individual point, as well as to the composite improvement number. The T4 improves 5.6% BSFC over the 2017MY development engine, or assuming at least 6.6% with the addition of the VWP.
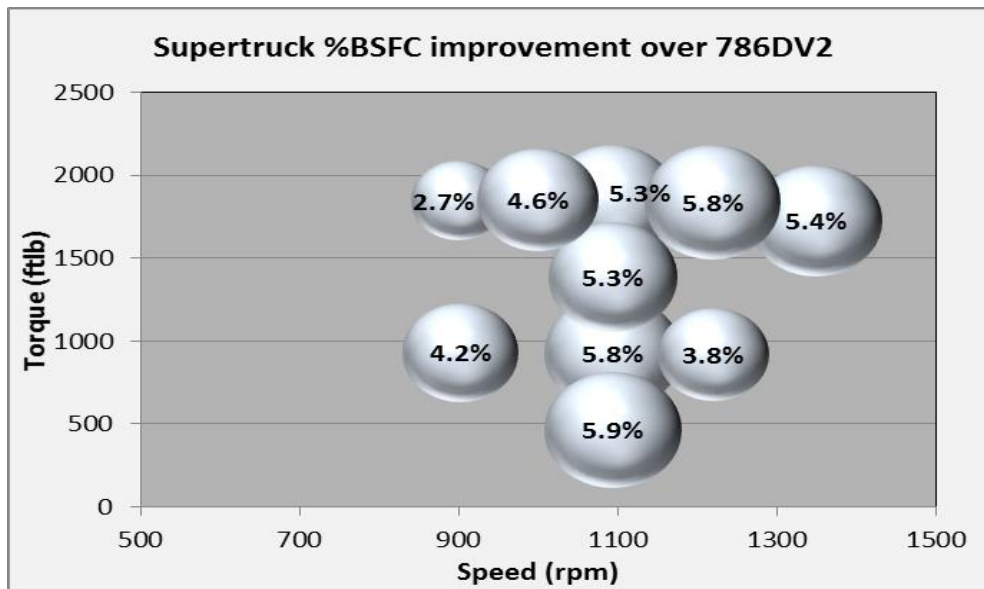
Figure 51: T4 BSFC improvement on the 10-point drive cycle sample over 2017MY

Figure 52: T4 Supertruck weight vs the 2009MY baseline mule, control vehicle

$$Freight\ Efficiency = Freight\ (Tons)\ @\ 65k\ GVW * MPG$$

⬇ Vehicle Weight ➜ ⬆ Freight while maintaining 65k GVW
⬆ Vehicle Efficiency ➜ ⬆ Vehicle miles per gallon

Scenario	Freight Efficiency (FE) Improvement	Weighting Factor*
A (Flat)	119%	38%
B (Hilly)	101%	38%
C (Urban)	88%	25%
Composite:		104%

* Composite weighting factors were determined at the beginning of the ST program and are DOE specific. Weighting factors reflect customer usage profiles across the entire product line (Class 6-8), not necessarily the Line Haul configuration tested.
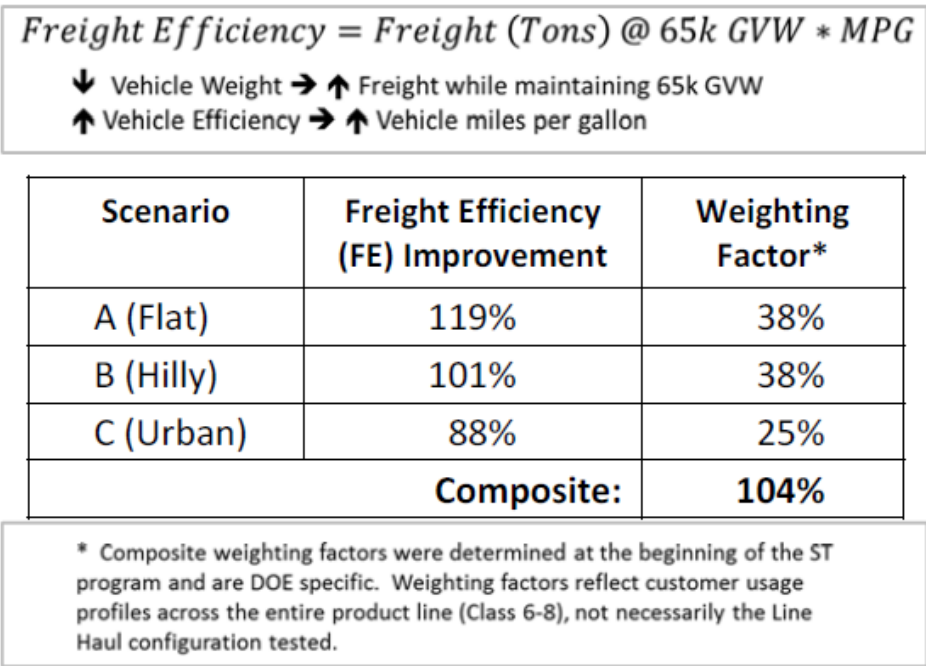
Figure 53: Contribution of freight efficiency improvement for each of the vehicle fuel economy tests for the T4 vehicle

Figure 52 shows a very interesting outcome from the T4 truck. As mentioned in this paper, there are many pieces of additional hardware to the T4, the large battery pack, and the WHR system for instance. However, with all the other weight reductions made, the Supertruck still comes out lighter than the control vehicle. This means that the T4 can be loaded with more freight. That weight reduction alone translates to an 8.5% improvement in freight efficiency. As a result of the work on the Supertruck program at Navistar, the total vehicle package was able to achieve a composite freight improvement of 104%, and could achieve over 13 miles per gallon. The contribution from each cycle ran with the T4 truck can be seen in **Figure 53**. On the Illinois Flatland cycle, the Superturck achieved a freight efficiency improvement of 119%.

The International Supertruck 1 exceeded the Department of Energy's goal of 80% freight efficiency improvement, and 50% BTE with 50.6% BTE. The efforts presented in the chapters of this paper proved to be successful in their goals of fuel economy improvement while maintaining global drivability of the vehicle, while still maintaining the Federal Emissions Limit of 0.2 BSNOx on the FTP and RMC. This was possible by wisely selecting the proper hardware and assembling a robust calibration meeting all of the constraints. This resulted in an over 11% improvement in the 50/50 drive cycle sample, from the 2009MY control vehicle: the point-wise improvement shown in in **Figure 54**.
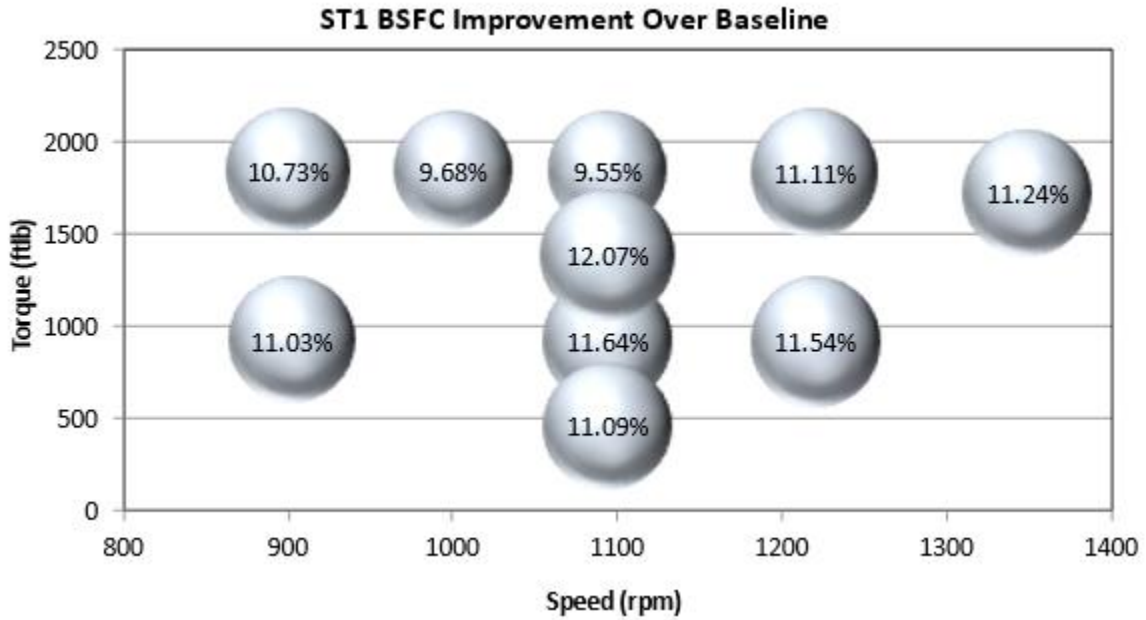
ST1 BSFC Improvement Over Baseline

Figure 54: Point-wise improvement on the 10-point 50/50 drive cycle sample of the final T4 engine calibration, over the 2009MY baseline

Moving forward for Supertruck 2 will be another 5-year program utilizing information gained from Supertruck 1, with new research for leading edge technologies required to meet the goal of 55% BTE. Considerable amounts of work are already being performed on increased turbo charger efficiencies which can directly improve BSFC. Other efforts like increasing heat release rate, decreasing combustion heat rejection, and other improvements to combustion will be a large portion of meeting the 55% BTE goal. The proposed waterfall shown in **Figure 55.**
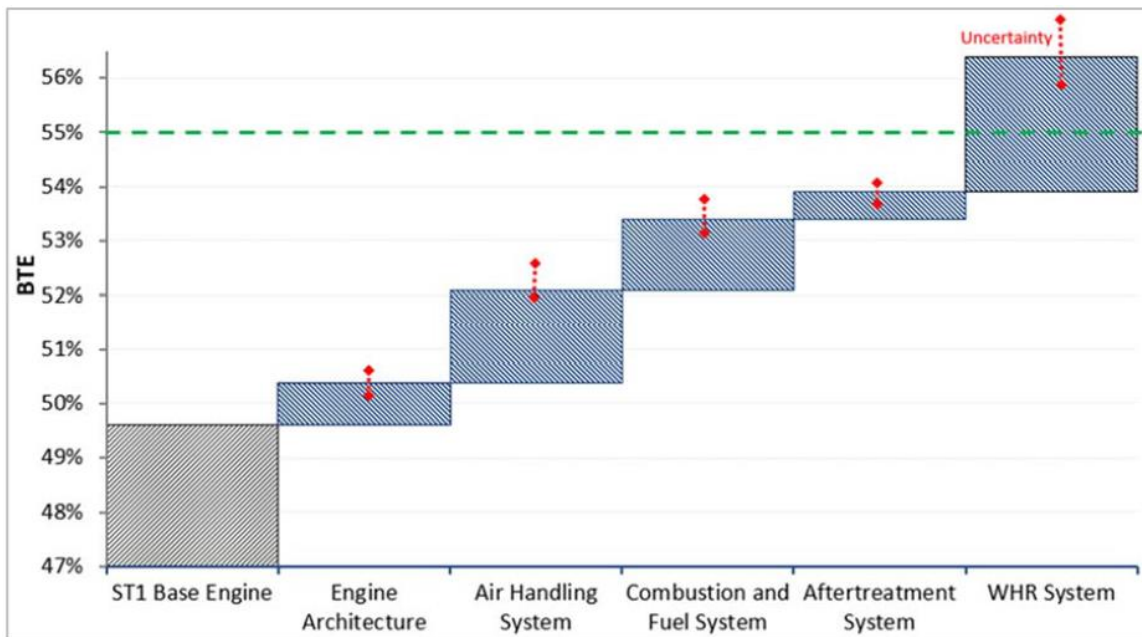

Figure 55: Proposed Supertruck 2 BTE improvements towards 55% BTE

References

Heywood, J. B. (1988). *Internal Combustion Engine Fundamentals*. Mc Graw Hill International Editions.

Pulkrabek, Willard W. *Engineering Fundamentals of the Internal Combustion Engine*. Prentice Hall, 1997.

"Thermodynamic Cycles." *Nuclear Power*, www.nuclear-power.net/nuclear-engineering/thermodynamics/thermodynamic-cycles

Ideal Rankine Cycle, home.iitk.ac.in/~suller/lectures/lec29.htm.

Navistar International*, Final Scientific/Technical Report For Supertruck Project: Development and Demonstration of a Fuel Efficient, Class 8 Tractor & Trailer Engine System*, 2016

Cìˍengel, Yunus A., and Michael A. Boles. *Thermodynamics: an Engineering Approach*. McGraw-Hill, 2011.

"Basic Principles of Vehicle Dynamics." *Brakes, Brake Control and Driver Assistance Systems: Function, Regulation and Components*, by Konrad Reif, Springer Vieweg, 2014.

Bandi, Keith E. "Fuel Efficiency Improvements in Heavy Truck Driveline Systems through Advanced Bearing Design and Technology." *SAE Technical Paper Series*, 2012, doi:10.4271/2012-36-0204.

Vojtech, Ryan. "Advanced combustion for improved thermal efficiency in an advanced on-road heavy duty diesel engine." *SAE Technical Paper Series*, 2018, https://doi.org/10.4271/2018-01-0237.

The Open Chamber Design Can Be Classified as Follows: • Semiquiescent ..., www.davuniversity.org/images/files/study-material/MEC258A-IC%20Engines-Combustion%20stage%20in%20CI%20Engine%20II.pdf. Accessed 2023.

Rajkumar, M., "Heat Release Analysis and Modeling for a Common-Rail Diesel Engine. " Master's Thesis, University of Tennessee, 2002. https://trace.tennessee.edu/utk_gradthes/2144

Finite Heat Release Model - University of Idaho, www.webpages.uidaho.edu/mindworks/IC_Engines/week%207/wK7_Heat%20Release%20Modeling.pdf. Accessed 2023.